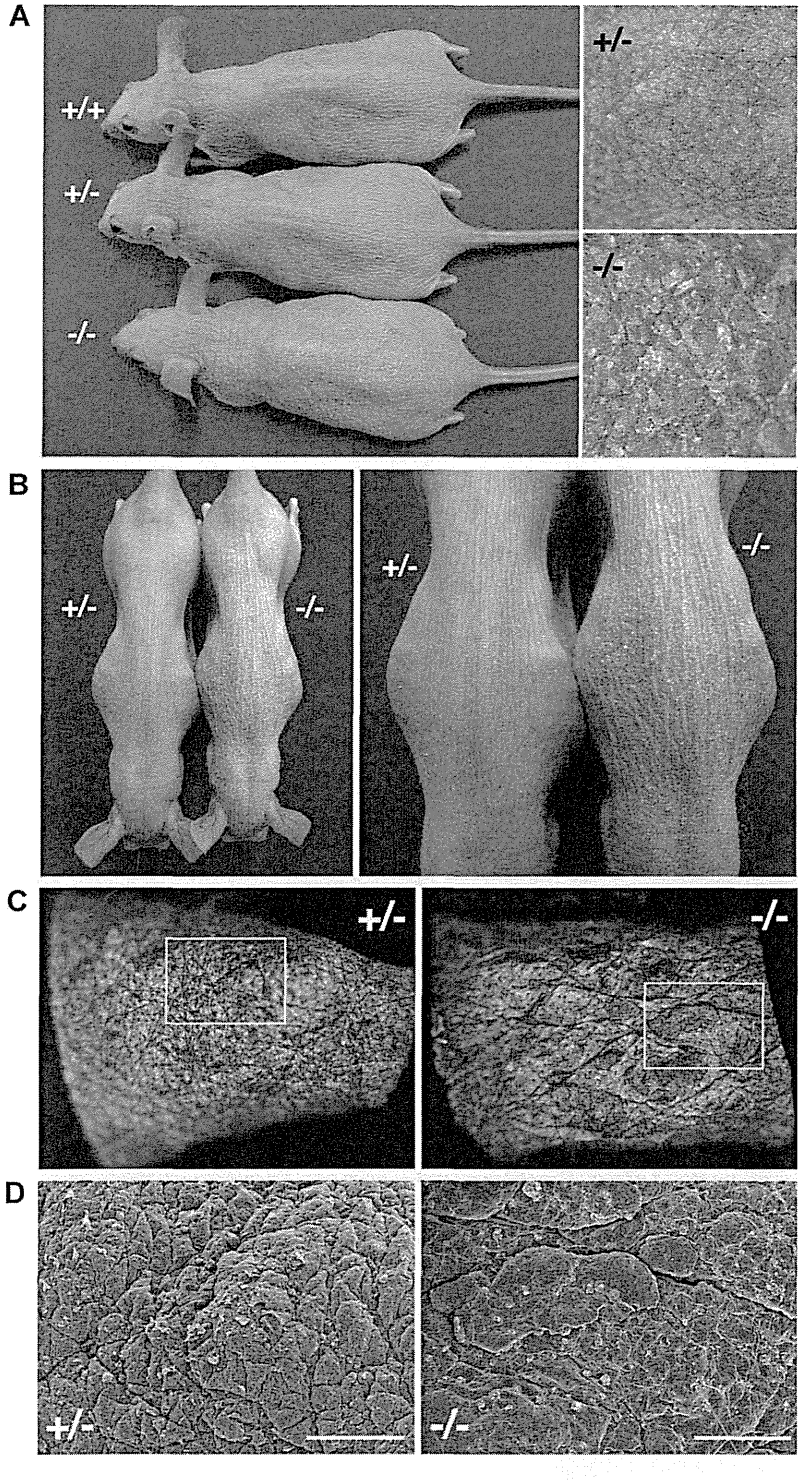

Figure 1. Morphological characterization of the epidermis of SASPase-deficient hairless mice.

A. Macroscopic observation of $SASP^{+/+}$, $SASP^{+/-}$ and $SASP^{-/-}$ hairless mice (left). Note that $SASP^{-/-}$ hairless mice showed drier and rougher skin. Stereomicroscopic examination of $SASP^{+/-}$ and $SASP^{-/-}$ hairless mice epidermis are also shown (right). Note that $SASP^{-/-}$ hairless mice had an epidermis with raised scales composed of many horny cells, whereas $SASP^{+/-}$ hairless mice had smooth, moist-looking skin with fine grooves.

B. Fine wrinkle formation in hung $SASP^{-/-}$ hairless mice. When hung by the tail, more wrinkles appeared on the surface of the back skin in $SASP^{-/-}$ hairless mice compared with $SASP^{+/-}$ hairless mice.

C. Stereomicroscopic examination of critical point dried epidermis of $SASP^{+/-}$ and $SASP^{-/-}$ hairless mice. In the $SASP^{+/-}$ hairless mice epidermis, many fine grooves were observed, whereas in the $SASP^{-/-}$ hairless mice, coarse grooves were observed. White boxes indicate the areas of interest investigated by SEM in D.

D. SEM of the epidermis of $SASP^{+/-}$ and $SASP^{-/-}$ hairless mice. In $SASP^{-/-}$ hairless mice, the intercellular spaces between horny cells could not be readily discerned, whereas individual horny cells were identified in their $SASP^{+/-}$ counterparts. Scale bars: 333 mm (left) and 375 mm (right).

phenotype than male mice (data not shown). Stereomicroscopic examination revealed that $SASP^{+/+}$ and $SASP^{+/-}$ mice had smooth, moist-looking skin with fine grooves, whereas $SASP^{-/-}$ hairless mice had skin with raised scales composed of many horny cells (Fig 1A right). When hung by their tails, more apparent differences were observed (Fig 1B). Specimens were fixed by standard techniques, dehydrated, dried at a critical point and examined employing scanning electron microcopy (SEM). After drying, epithelial scales of the skin of the $SASP^{+/-}$ hairless mice had fallen off, exposing the surface structure and resulting in many fine grooves. In contrast, coarse grooves were observed in the $SASP^{-/-}$ hairless mice (Fig 1C). Similarly, SEM revealed that the individual horny cells were easily identified in $SASP^{+/-}$ hairless mice, whereas the intercellular spaces between the horny cells could not be readily discerned in their $SASP^{-/-}$ counterparts (Fig 1D).

Morphology of SASP$^{-/-}$ mice epidermis

Next, we examined the histological analysis of SASP$^{-/-}$ hairless mice. The epidermis of the SASP$^{-/-}$ mice showed a normal layer organization of keratinocytes, and keratohyalin-granules were observed in both SASP$^{+/+}$ and SASP$^{-/-}$ mice at the level of hematoxylin–eosin (HE)-stained paraffin section images (Fig 2A and B). However, the cornified cells of the SASP$^{-/-}$ SC were compacted more tightly, and the number of layers was increased compared with SASP $^{+/+}$ mice (Fig 2A and B). Ultrathin section electron microscopy confirmed these findings at a higher resolution (Fig 2C–G). The appearance of individual cells from the SB to SS was indistinguishable between the SASP$^{+/+}$ and SASP$^{-/-}$ skin, and the SG contained both F- and L-granules in the SASP$^{-/-}$ SC (Fig 2C and D). Furthermore, the SC of SASP$^{-/-}$ mice showed 7–10 layers of electron dense and tightly compacted cell layers compared with that of SASP$^{+/+}$, which usually exhibited 5–7 layers (Fig 2C–H). These results suggest that a deficiency of SASPase in hairless background mice induced an abnormality in the SC.

Physiological features of SASP$^{-/-}$ epidermis

To physiologically characterize the epidermal surface of the SASP$^{-/-}$ hairless mice, we measured the trans-epidermal water loss (TEWL) and the SC hydration of SASP$^{+/+}$ ($n=7$) and SASP$^{-/-}$ ($n=11$) mice (Fig 3A and B). Although the TEWL was not significantly changed between SASP$^{+/+}$ and SASP$^{-/-}$ mice (Fig 3A), a clear difference was observed in SC hydration. As such, SC hydration of SASP$^{-/-}$ mice was significantly lower than in SASP$^{+/+}$ mice (Fig 3B). These results indicate that SASP$^{-/-}$ hairless mice showed markedly decreased SC hydration without alteration of barrier function.

Aberrant profilaggrin processing in SASP$^{-/-}$ hairless mice

Next, to analyse the epidermal differentiation of SASP$^{-/-}$ hairless mice, the expression of various epidermal differentiation markers were examined. Immunofluorescence staining of frozen sections of back skin epidermis with anti-keratin 14, keratin 1, involucrin and loricrin pAbs revealed normal

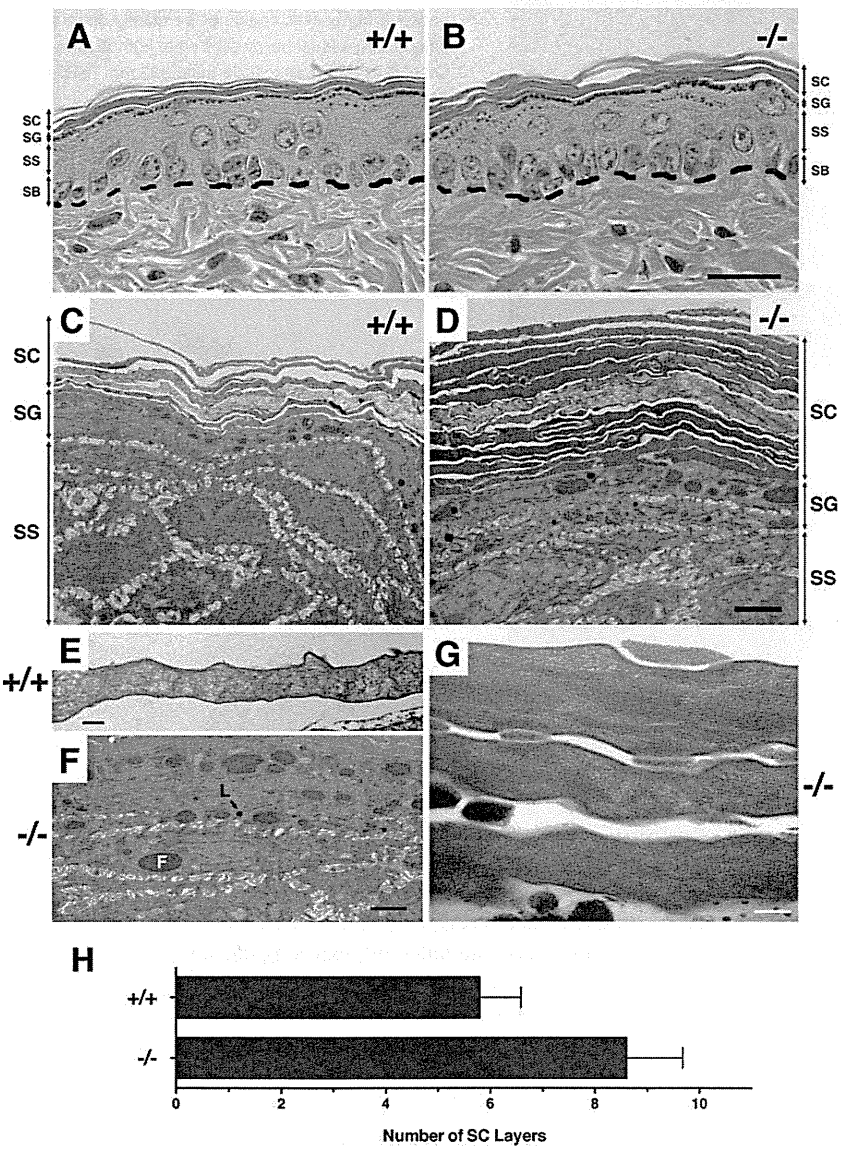

Figure 2. SASP$^{-/-}$ hairless mouse epidermis showed an increased number of layers in the aberrant SC.

A, B. Sections of SASP$^{+/+}$and SASP$^{-/-}$epidermis examined by HE staining. HE staining of SASP$^{-/-}$ hairless mice showed a marked thickening of the SC with an increased number of layers compared with SASP$^{+/+}$ mice. Scale bar: 100 μm.

C, D. Sections of SASP$^{+/+}$ and SASP$^{-/-}$epidermis examined by electron microscopy. TEM analysis of SASP$^{+/+}$ and SASP$^{-/-}$ epidermis showed an increased number of electron dense layers in the SC of SASP$^{-/-}$ mice compared with SASP$^{+/+}$ mice. Scale bar: 4 μm.

E. Typical layers of the SC of SASP$^{+/+}$ hairless epidermis. Scale bar: 500 nm.

F. The granular layer of the SASP$^{-/-}$ hairless mice. Both F-granules (F) and L-granules (L) were observed, suggesting that keratohyalin granule formation normally occurs in SASP$^{-/-}$ hairless mice. Scale bar: 2 μm.

G. Typical electron dense layers of the SC of SASP$^{-/-}$ hairless epidermis. Scale bar: 100 nm.

H. The number of layers in the SC of SASP$^{+/+}$ and SASP$^{-/-}$ epidermis were counted in five independent areas/mouse in the TEM images of two female mice. The average number of layers in the SC was 5.8 ± 0.8 SD and 8.6 ± 1.07 SD in SASP$^{+/+}$ and SASP$^{-/-}$ epidermis, respectively.

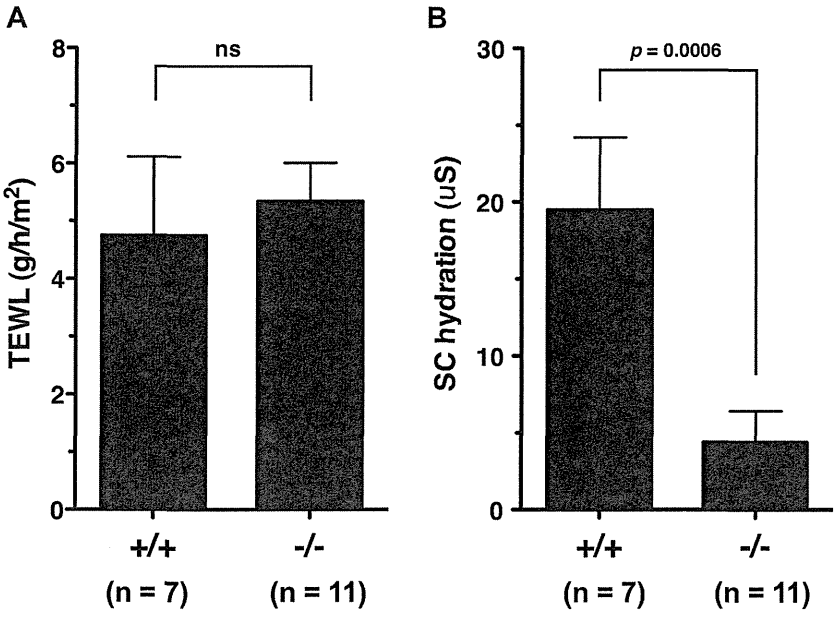

Figure 3. SASPase regulates SC hydration.

A. Trans-epidermal water loss (TEWL) of $SASP^{+/+}$ and $SASP^{-/-}$ hairless mice. TEWL of hairless mice were measured using VAVO SCAN (Asahi Biomed, Tokyo, Japan). The TEWL of $SASP^{-/-}$ hairless mice was not significantly changed. The numbers of animals tested were: $SASP^{+/+}$, $n = 7$ and $SASP^{-/-}$, $n = 11$. ns: not significant (Mann Whitney test on mean values ± SD using Graphpad software).

B. SC hydration levels of $SASP^{+/+}$ and $SASP^{-/-}$ hairless mice. SC hydration levels of hairless mice were measured using ASA-M1 (Asahi Biomed). The SC hydration of $SASP^{-/-}$ hairless mice was significantly lower than that of $SASP^{+/+}$ hairless mice. The numbers of animals tested were: $SASP^{+/+}$, $n = 7$ and $SASP^{-/-}$, $n = 11$. The p value is indicated above the bar (Mann Whitney test on mean values ± SD using Graphpad software).

expressions and localization of epidermal differentiation markers (Supporting information Fig 2A). Immunoblotting of back skin epidermal urea extracts with anti-keratin 14, keratin 1, involucrin and loricrin pAbs also revealed that the corresponding expression levels were not altered (Supporting information Fig 2B). On the other hand, immunofluorescence staining with anti-filaggrin pAb revealed that filaggrin-positive layers of the SC (lower SC) were increased in the back skin epidermis of the $SASP^{-/-}$ hairless mice (Fig 4A and B). To carefully compare the filaggrin in the lower SC, we tape-stripped the SC of the $SASP^{+/-}$ and $SASP^{-/-}$ epidermis. Coomassie brilliant blue (CBB) staining of equivalent amounts of the extracts revealed that all the major bands were decreased, suggesting there were increased concentrations of certain smear proteins (Fig 4C, left). Immunoblotting of the same samples with anti-filaggrin pAb revealed the accumulation of primarily two smear bands below the size of dimeric and trimeric filaggrin and that a mature filaggrin band was rarely detected (Fig 4C, right). These results suggest that a deficiency of SASPase resulted in the accumulation of premature processed dimeric and trimeric filaggrin and that mouse SASPase cleaves the linker sequence of mouse profilaggrin *in vivo*. The processing of mouse profilaggrin in the C57BL/6J mouse was reported to occur in a two-step process via two types of profilaggrin linker sequences with or without FYPV, respectively (Resing et al, 1989). First, a profilaggrin linker sequence containing FYPV may be cleaved, resulting in the accumulation of a two-domain intermediate (2DI) and a three-domain intermediate (3DI). Second, the linker type without FYPV, which connects 2DI and 3DI of monomeric filaggrin, is potentially cleaved by a Ca^{2+} dependent protease (Resing et al, 1989, 1993a). Some amino acid residues are then removed from the exposed sites by further exoprotease activity (Resing et al, 1989). Therefore, accumulation of dimeric and trimeric-like profilaggrin in the $SASP^{-/-}$ epidermis in Hos:HR-1 background suggests that SASPase may be involved in either the first or second processing steps.

SASPase directly cleaves the profilaggrin linker sequence *in vitro*

Accumulation of aberrant dimeric and trimeric profilaggrin in the lower SC of the $SASP^{-/-}$ hairless mice implies that the profilaggrin linker peptide is a direct substrate for SASPase. To confirm this hypothesis, we examined whether SASPase directly cleaves the profilaggrin linker peptide *in vitro*. Because it was difficult to produce recombinant mouse filaggrin with a linker peptide in *Escherichia coli* because of excess degradation, we produced human filaggrin (hFilaggrin) as a fusion protein of maltose binding protein (MBP) connected with the human profilaggrin linker peptide in *E. coli*. Purified MBP-hFilaggrin showed a triple banding pattern. The N-terminal amino acid sequence of the major upper two bands revealed that both proteins had an intact N-terminus of MBP indicating that C-terminally processed filaggrin (MBP-hFilaggrin-ΔC) was copurified with MBP-hFilaggrin. To prepare the active form of SASPase (14 kDa; hSASP14; 191-326aa), we expressed and purified a 28 kDa form of human SASPase (hSASP28; 85-343aa) as a fusion protein with GST (GST-hSASP28) in *E. coli* (Bernard et al, 2005). After complete autoprocessing under weakly acidic conditions (pH 6.0), which is the optimum pH of SASPase, the produced hSASP14 was purified (Fig 5A; Bernard et al, 2005; Matsui et al, 2006). Next, hSASP14 was incubated with MBP-hFilaggrin/-hFilaggrin-ΔC under weakly acidic conditions (pH 6.0). As shown in Fig 5B, MBP-hFilaggrin/hFilaggrin-ΔC was cleaved into mainly 42, 37 and 23 kDa proteins (Fig 5B and C). The 42 kDa protein was recognized by anti-MBP pAb (data not shown), and the N-terminal amino acid sequencing confirmed that the protein at 42 kDa was the MBP protein itself. The N-terminal amino acid sequencing of the 37 and 23 kDa identified the same peptide, 'QVSTH'. This N-terminal amino

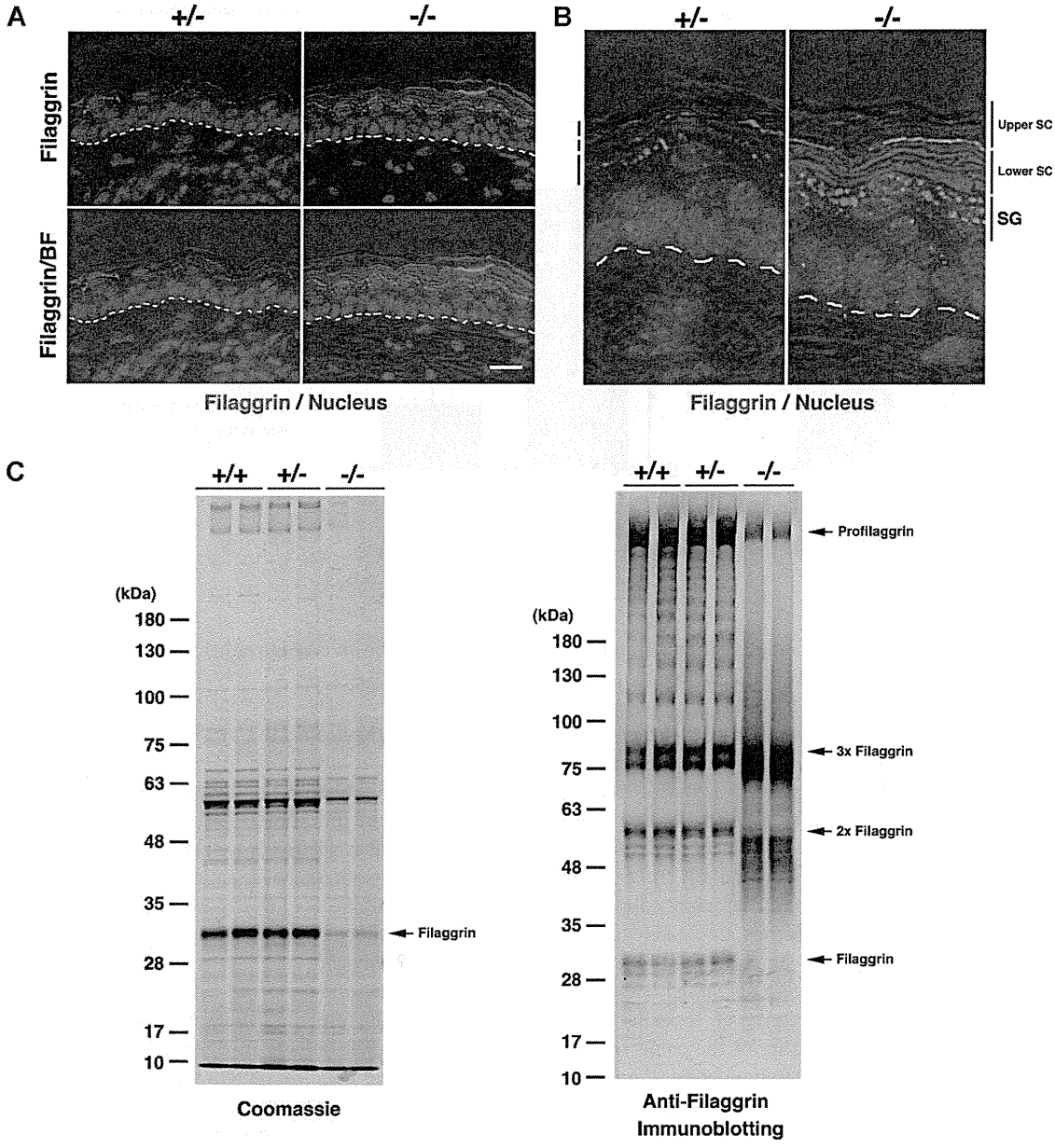

Figure 4. Aberrant expression of filaggrin in SASP$^{-/-}$ hairless mice.

A. Immunofluorescence staining of frozen sections of the back skin of SASP$^{+/-}$ and SASP$^{-/-}$ mice stained with anti-filaggrin antibody (red). Nuclei were counterstained with bisbenzimide (blue). The SASP$^{-/-}$ epidermis showed an increased amount of filaggrin-positive stained lower SC. Dashed lines represent the border between the epidermis and dermis. *BF*, bright field. Scale bar: 10 μm.

B. Enlarged view of A shows an increased amount of lower SC layers in the SASP$^{-/-}$ hairless epidermis.

C. Equivalent amounts of tape-stripped extracts (10 times, 5 μg) from SASP$^{+/+}$ ($n = 2$), SASP$^{+/-}$ ($n = 2$), and SASP$^{-/-}$ ($n = 2$) mice were immunoblotted with anti-filaggrin antibodies. CBB staining of extracts revealed a reduced expression of filaggrin monomer bands and other major SC proteins in the SASP$^{-/-}$ hairless mice epidermis (left; Coomassie). Immunoblotting with anti-filaggrin demonstrated that an accumulation of aberrant filaggrin degradation products (dimer and trimer sized) was detected (right), whereas mature filaggrin was rarely detected. As equivalent amounts of SC extracts were loaded, the intensity of the profilaggrin band was decreased in SASP$^{-/-}$, possibly due to an increase in the concentrations of other smear proteins.

acid sequence corresponded to the previously reported N-terminal amino acid sequence of native monomeric human filaggrin, in which Q is modified into pyrrolidone carboxylic acid (PCA) (Thulin & Walsh, 1995; Thulin et al, 1996). These results indicate that hSASP14 cleaved MBP-hFilaggrin and produced MBP (42 kDa) and hFilaggrin (37 kDa), of which the N-terminus was QVSTH. Furthermore, MBP-hFilaggrin-ΔC was cleaved at the same site and produced MBP (42 kDa) and hFilaggrin-ΔC (23 kDa), of which the N-terminus was QVSTH (Fig 5B and C). Thus, we conclude that hSASP14 cleaved the linker sequence

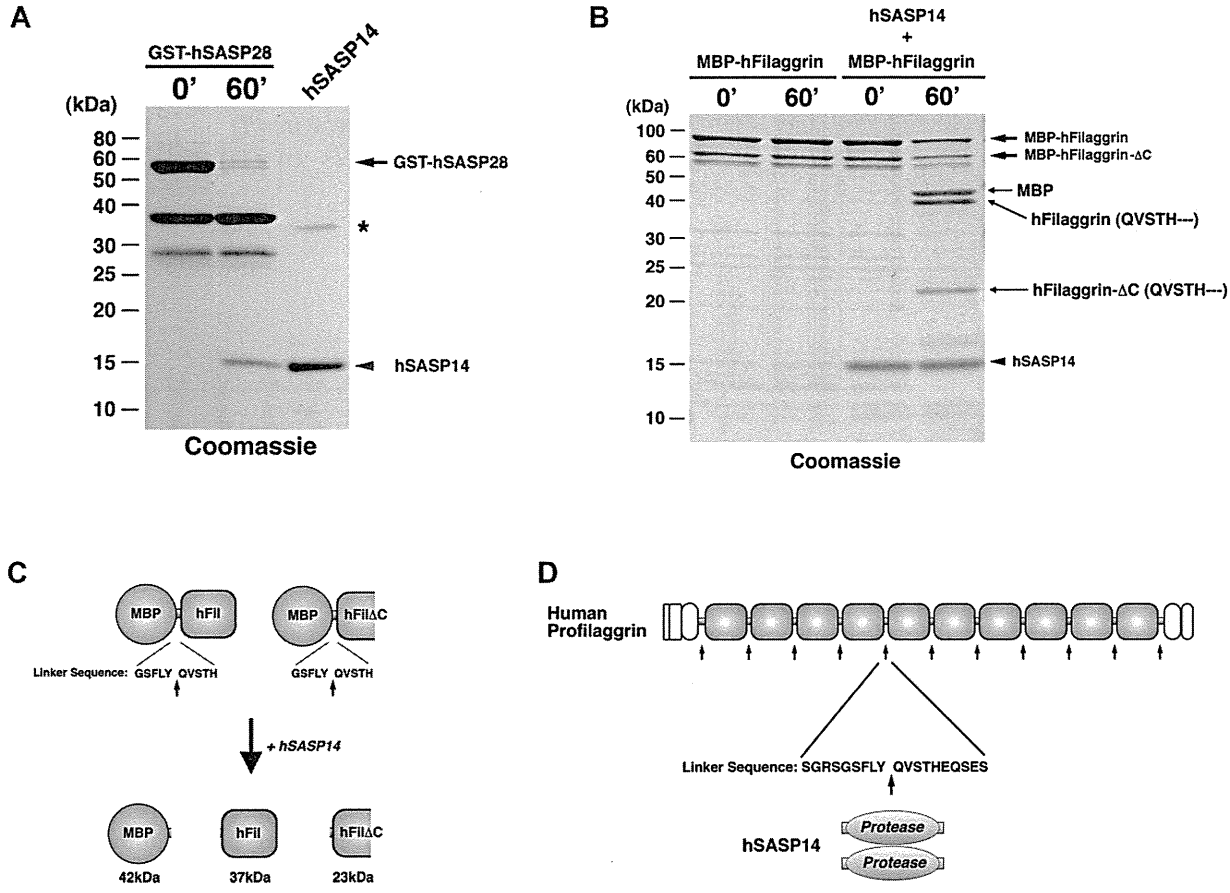

Figure 5. Recombinant hSASP14 directly cleaves recombinant filaggrin *in vitro*.

A. Production and purification of hSASP14 by autoprocessing of GST-hSASP28. Purified GST-hSASP28 (arrow) was incubated for the indicated times (0′, 0 min; 60′, 60 min) with 700 mM NaCl at pH 6.0. GST-hSASP28 underwent autoprocessing and produced hSASP14 (arrowhead). Cleaved GST-fusion proteins were removed by passing through Glutathione Sepharose 4B beads to purify hSASP14 (arrowhead). Asterisk indicates a dimer of hSASP14.

B. Cleavage of profilaggrin linker peptide by hSASP14 *in vitro*. The purified MBP-hFilaggrin/MBP-hFilaggrin-ΔC (arrow) was incubated with or without the purified hSASP14 (arrowhead) with 700 mM NaCl at pH 6.0 for 60 min at 37°C. The linker peptide of profilaggrin between MBP and hFilaggrin in MBP-hFilaggrin/MBP-hFilaggrin-ΔC was cleaved by hSASP14, resulting in the production of MBP (42 kDa), hFilaggrin (37 kDa), and hFilaggrin-ΔC (23 kDa). The N-terminal amino acid sequencing of hFilaggrin (37 kDa) and hFilaggrin-ΔC (23 kDa) protein identified QVSTH amino acids, which corresponded to the linker peptide of profilaggrin.

C. Schematic representation of the mode of processing of MBP-hFilaggrin by hSASP14 as described in B.

D. Schematic representation of the possible cleavage site of profilaggrin by hSASP14. Homodimerized hSASP14 proteins were suggested to primarily cleave between GSFLY-QVSTH in the profilaggrin linker sequence (arrow).

of human profilaggrin between 'GSFLY' and 'QVSTH' *in vitro* (Fig 5C and D).

Normal free amino acid composition in SC of SASP$^{-/-}$ mice

Previous reports suggest that NMFs serve as natural humectants of SC (reviewed in Rawlings & Matts, 2005). To investigate whether aberrant processing of filaggrin had a detrimental effect on the composition of NMFs, we performed free amino acid analysis of tape stripped SC of SASP$^{+/+}$ ($n=7$) and SASP$^{-/-}$ ($n=11$) mice. There were no alterations in the total amount or the composition of free amino acids (Fig 6A and B). These results suggest the NMFs were normal in SASP$^{-/-}$ SC, despite the marked decrease in SC hydration.

Mutations of human SASPase affect autoprocessing and profilaggrin linker cleavage activity

Analysis of our SASP$^{-/-}$ hairless mice indicates that loss of SASPase activity may result in dry skin accompanied by an accumulation of unprocessed profilaggrin. Thus, we investigated whether the human genome possesses SASPase mutations, which consequently affect protease activity, i.e. profilaggrin to filaggrin processing activity. We investigated mutations in the SASPase gene in 28 control subjects and 196 AD-patients (Sasaki et al, 2008). As a result of the mutation search on the human SASPase gene, two types of missense mutations (D232Y and V243A: 3.5% [1/28]) in the control subjects, four types of missense mutations (A54S: 0.5% [1/196],

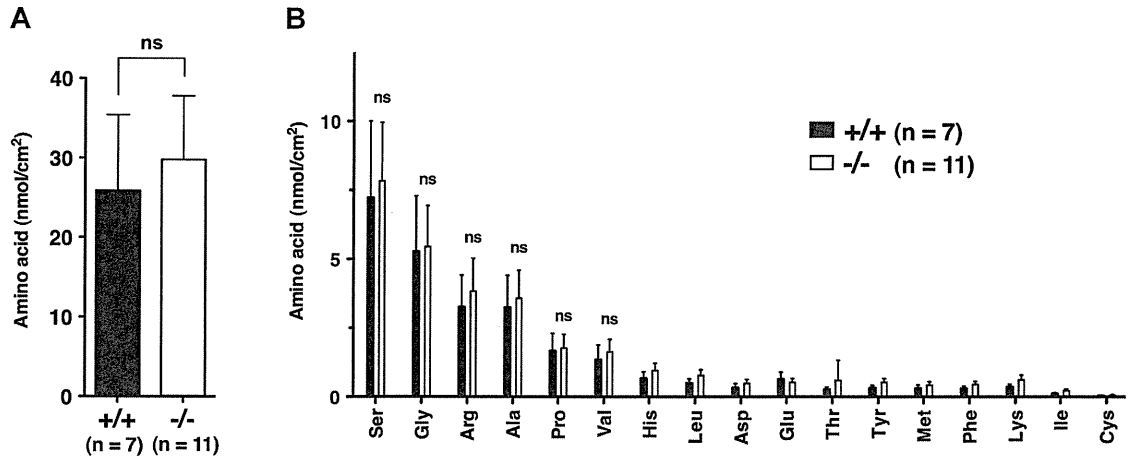

Figure 6. Free amino acids in SC of SASP$^{+/+}$ and SASP$^{-/-}$ mice.

A. Total free amino acid composition analysis. Tape stripped SC of SASP$^{+/+}$ ($n = 7$, filled column) and SASP$^{-/-}$ ($n = 11$, open column) hairless mice were subjected to amino acid analysis. Total free amino acid composition analyses showed no difference between the SC of SASP$^{+/+}$ and SASP$^{-/-}$ mice. ns: not significant (Mann–Whitney test on mean values ± SD using Graphpad software).

B. Individual free amino acid composition analysis. Individual free amino acid composition analyses also showed no difference between the SC of SASP$^{+/+}$($n = 7$, filled columns) and SASP$^{-/-}$ mice ($n = 11$, open columns). ns: not significant (Mann–Whitney test on mean values ± SD using Graphpad software).

I186T: 0.5% [1/196], V187I: 1.5% [3/196], R311C: 0.5% [1/196]), and three types of silent mutations (F101F: 0.5% [1/196], P206P: 3.1% [6/196], N276N: 1.5% [3/196]) in the AD patients were identified (Fig 7A, Supporting information Tables I and II). All mutations were heterozygous. V187I was most frequently identified (identified in three AD patients). A54S and R311C were found in the same patient and in the same allele. The number of patients and mutation types are shown in Supporting information Tables I and II.

To examine whether these mutations affect the protease activity of SASPase, we bacterially expressed and purified GST-hSASP28 bearing the mutations I186T, V187I, R311C, D232Y, or V243A, and performed an *in vitro* autoprocessing assay as previously described (Bernard et al, 2005; Matsui et al, 2006). To compare the autoprocessing activity *in vitro*, we purified GST-hSASP28 mutants (Fig 7B). We could not examine the autoprocessing activity of GST-hSASP28(I186T)/(R311C), because full-length GST-hSASP28(I186T)/(R311C) was barely purified, possibly due to the higher autoprocessing activity in *E. coli*. The rest of the purified GST-hSASP28(WT)/(D232Y)/(V243A) was incubated under weakly acidic conditions (pH 6.0), which is the optimal pH of SASPase (Bernard et al, 2005; Matsui et al, 2006). As shown in Fig 7C, GST-hSASP28(D232Y) showed autoprocessing activity similar to that of the WT, and V243A showed no autoprocessing activity.

We next examined whether the V187I mutation, which was identified most frequently in AD patients (three patients), affected autoprocessing activity *in vitro*. The purified GST-hSASP28(WT)/(V187I) was incubated under weakly acidic conditions (pH 6.0). As shown in Fig 7D, GST-hSASP28(V187I) showed decreased autoprocessing activity in both 300 and 400 mM NaCl. Fig 7E shows the time course by semi-quantification of produced hSASP14. Because V187I is located outside of the cleaved hSASP14, autoprocessed hSASP14 from hSASP28(V187I) should be the same as the WT. Therefore, the initial autoprocessing reaction (1–30 min in 300 mM NaCl) should reflect the difference between WT and V187I. The reaction rate of GST-hSASP28(V187I) at 300 mM NaCl was estimated at 5.6-fold over 15–30 min, which is lower than that of GST-hSASP28(WT). These results indicate that hSASP28(V187I) has substantially reduced activity at pH6.0 *in vitro* compared to WT. Finally, we examined whether the V187I mutation had an effect on the filaggrin linker cleavage activity of GST-hSASP28 *in vitro*. To examine whether the mutation of V187I affected the profilaggrin cleavage activity, we incubated GST-hSASP28(WT) or GST-hSASP28(V187I) with MBP-hFilaggrin/MBP-hFilaggrin-ΔC under weakly acidic conditions (pH 6.0). As expected, the MBP-hFilaggrin cleavage activity by GST-hSASP28 was suppressed in GST-hSASP28(V187I) compared with GST-hSASP28(WT), relative to the production of hSASP14 (Fig 7E). These results indicate that GST-hSASP28(V187I) showed decreased autoprocessing activity at pH 6.0, resulting in decreased profilaggrin linker cleavage activity *in vitro*.

It is important to elucidate whether these heterogenic loss-of-function mutations of SASPase affect human skin physiology. And it is possible there was some dry skin in our non-AD cohort as criteria of this cohort did not discriminate against dry skin (Sasaki et al, 2008). We measured TEWL and SC hydration of a non-AD individual with a mutation (V243A/+) as well as three normal individuals without mutations. The appearance of the skin surface, TEWL and SC hydration of V243A/+ were similar to the three normal individuals (Supporting information Fig 3). These results did not provide conclusive evidence due to the small numbers tested. In the case of complex disorders like AD, it is difficult to prove a direct role of the sequence variant in the

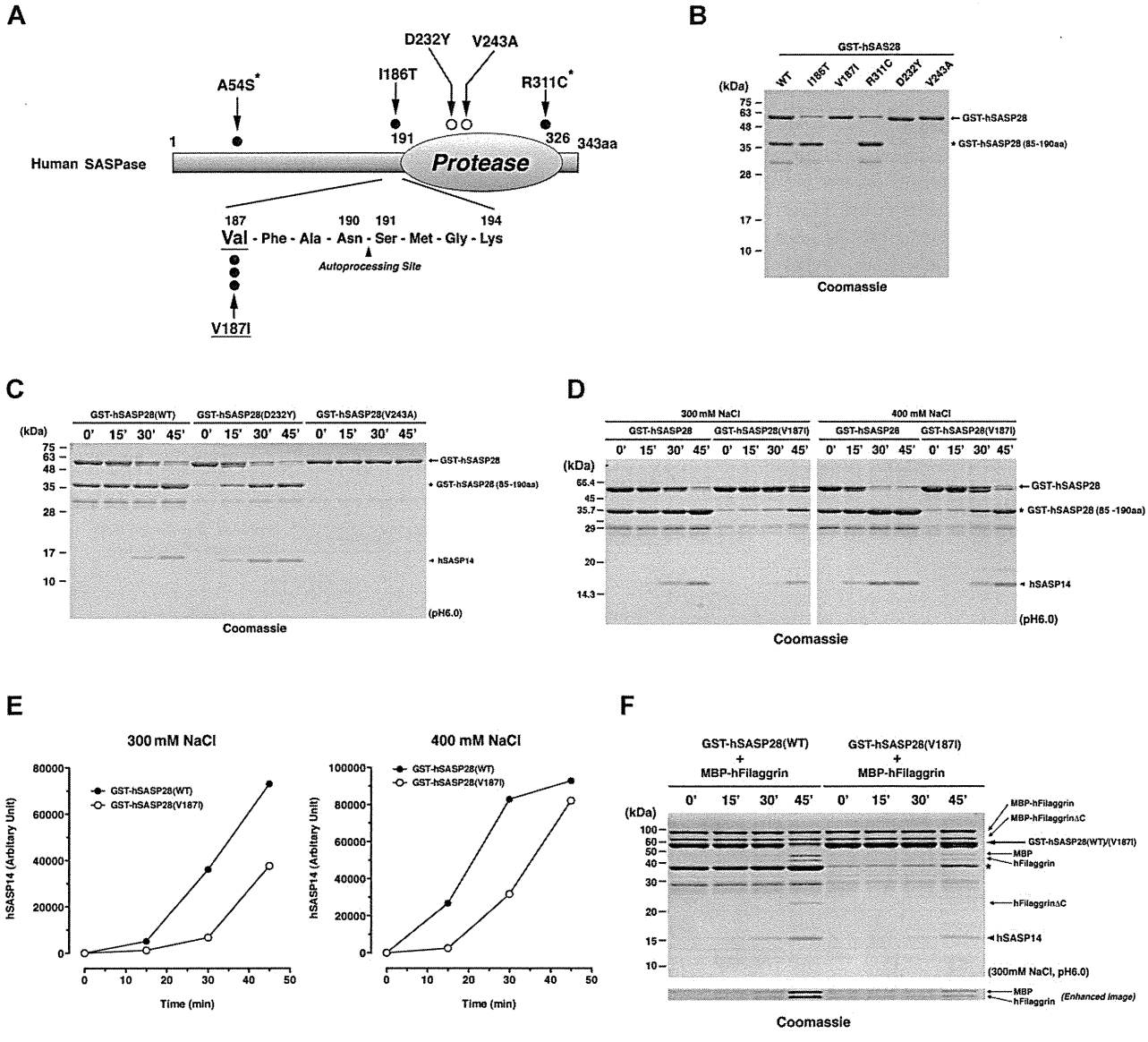

Figure 7. Biochemical characterization of human mutations in SASPase.

A. Schematic representation of human mutations identified in AD patients ($n = 196$; closed circles) and case controls ($n = 28$; open circles). The amino acid sequence of the autoprocessing site (between Asn^{190} and Ser^{191}) is indicated. Asterisks of A54S and R311C indicate that these mutations were found in the same patient and in the same allele.

B. Purification of GST-hSASP28 mutants. Purified GST-hSASP28 (WT)/(I186T)/(V187I)/(R311C)/(D232Y)/(V243A) (1 μg) were subjected to SDS-PAGE and stained with CBB. GST-hSASP28 (V187I) and (V243A) did not produce any partially cleaved products. Arrow indicates GST-hSASP28. Asterisk indicates the partially cleaved product of N-terminal hSASP28 (85-190aa) fused with GST (see A).

C. Comparison of autoprocessing activity among GST-hSASP28(WT), (D232Y) and (V243A). 1.4 mg/ml of GST-hSASP28(WT), (D232Y) and (V243A) were incubated at pH 6.0 for indicated times and subjected to SDS-PAGE and stained with CBB. The autoprocessing activity of GST-hSASP28(D232Y) was comparable to that of GST-hSASP28(WT), whereas GST-hSASP28(V243A) did not show any autoprocessing activity *in vitro*. Arrowhead indicates the hSASP14.

D. Comparison of autoprocessing activity between GST-hSASP28(WT) and (V187I). 0.9 mg/ml of GST-hSASP28(WT) and (V187I) were incubated under 300 or 400 mM NaCl at pH 6.0 for indicated times, subjected to SDS-PAGE, and stained with CBB. The autoprocessing activity of GST-hSASP28(V187I) was weaker than that of GST-hSASP28(WT) in both conditions.

E. Reaction curve of GST-hSASP28(WT) and (V187I) autoprocessing. Autoprocessed hSASP14 from GST-hSASP28(WT) (closed circles) and GST-hSASP28(V187I) (open circles) in Fig 8D was semi-quantified from a gel image. The reaction rate was higher in 400 mM (right) than in 300 mM NaCl (left). V187I mutation affected the initial reaction rate and showed 5.6-fold reduced activity over 15–30 min in 300 mM NaCl.

F. Comparison of profilaggrin linker peptide cleavage activity between GST-hSASP28(WT) and (V187I). 0.9 mg/ml of GST-hSASP28(WT) and (V187I) were incubated with 0.4 mg/ml of MBP-hFilaggrin/MBP-hFilaggrin-ΔC under 300 or 400 mM NaCl at pH 6.0 for the indicated times, subjected to SDS-PAGE, and stained with CBB. The profilaggrin linker cleavage activity was weaker in GST-hSASP28(V187I) than in that of (WT), relative to the production of hSASP14 by autoprocessing. An enhanced image of the MBP and hFilaggrin band areas is also shown.

pathogenesis. In the future, it is necessary to perform a large-scale cohort analysis to clarify the clinicopathological significance of SASPase mutation.

Physiological role of SASPase

Figure 8 summarizes our findings. In normal epidermis, non-phosphorylated profilaggrin is orderly processed into filaggrin and bundle keratin filaments at the 'lower SC', then degraded into free amino acids which constitute most of the NMFs in the 'upper SC'. SASPase deficiency causes incomplete linker cleavage of profilaggrin resulting in an accumulation of trimeric and dimeric profilaggrins slightly degraded from either N- or C-terminal ends in the 'lower SC'. Such aberrant profilaggrin may bind to keratin filaments, finally degrade, and produce a normal composition of free amino acids in the 'upper SC'. Finally, the SC of SASP$^{-/-}$ epidermis has an increased number of layers and produces a wrinkled, dry, rough skin.

DISCUSSION

In our previous study, we reported increased fine wrinkles at the side of the body in SASP$^{-/-}$ mice raised on a C57BL/6J background. However, we were not able to distinguish any morphological changes between SASP$^{+/-}$ and SASP$^{-/-}$ mice, possibly due to the thin epidermis of the back skin (Matsui et al, 2006). In this paper, we generated SASP$^{-/-}$ mice with Hos:HR-1 background. The increased thickness of the epidermis of these mice enabled us to distinguish a clear difference in SC structure and profilaggrin processing pattern in the SC. SASP$^{-/-}$ hairless mice showed a marked decrease in SC hydration and an increased number of electron dense layers in the SC. Such aberrant layers in the SC consisted of an upper SC without filaggrin staining and a lower SC stained by anti-filaggrin Ab with the accumulation of aberrant dimeric and trimeric filaggrin, i.e. premature profilaggrin processing (Figs 5B and 8). Interestingly, the composition

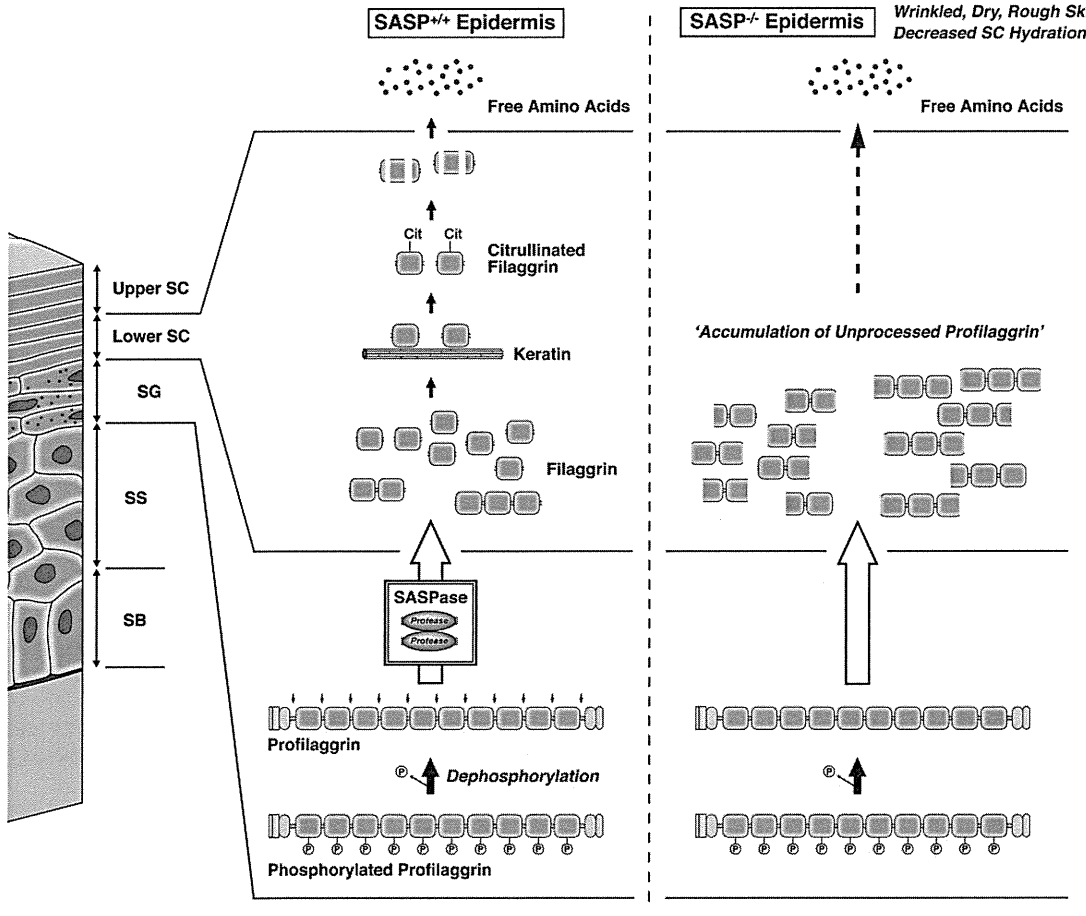

Figure 8. Schematic representation of the possible profilaggrin processing pathway observed in the SASP$^{+/+}$ and SASP$^{-/-}$ epidermis. In the SASP$^{+/+}$ epidermis, highly phosphorylated profilaggrin expressed in the SG is dephosphorylated in the upper most SG. The linker sequence that connects each filaggrin monomer is then cleaved by SASPase at the SG-to-SC transition via production of two kinds of intermediates (2DI and 3DI). Monomeric filaggrin strongly binds to keratin filaments in the lower SC to form bundled keratin filaments. After citrullination, filaggrin is released from keratin and further degraded to form free amino acids, which constitute most of the NMFs in the upper SC. In the SASP$^{-/-}$ epidermis, trimeric and dimeric profilaggrins slightly degraded from either N- or C-terminal ends, accumulate because of incomplete linker sequence cleavage. Aberrantly processed profilaggrin binds to keratin filaments and degrades into free amino acids without the production of monomeric filaggrin. Finally, aberrant SC causes wrinkled, dry, rough skin with decreased SC hydration. SC, stratum corneum; SG, stratum granulosum; SS, stratum spinosum; SB, stratum basale.

and quantity of major free amino acids were not altered in the dry skin-like SC of SASP$^{-/-}$ hairless mice (Fig 6).

Hydration of the SC plays an important role in maintaining metabolic activity, enzyme activity, mechanical properties, appearance and barrier function of the skin and is dependent on (i) organization of the tight and semi-permeable barrier of intercellular lamellar lipids, (ii) the diffusion path length created by the SC layers and corneocyte envelopes, and (iii) the presence of NMFs (Rawlings & Harding, 2004; Rawlings & Matts, 2005). NMFs comprise up to 10% of the SC and are reported to be an important natural humectants of the SC because of their hygroscopic features (Rawlings & Harding, 2004; Rawlings & Matts, 2005). Most NMFs are composed of free amino acids derived from the degradation products of filaggrin and its derivatives, PCA and urocanic acid (UCA). There are also non-amino-acid-derived (non-filaggrin-derived) NMFs, such as sugars, hyaluronic acid, urea, citrate, lactate, and glycerol (Fluhr et al, 2008; Rawlings & Harding, 2004; Rawlings & Matts, 2005). Although we did not analyse the PCA or UCA of SASP$^{-/-}$ hairless mice, there were no changes in free amino acids, which suggests that filaggrin-derived NMFs were not altered. The accumulation of aberrantly processed profilaggrin without monomer filaggrin in the 'lower SC' accompanied by a normal free amino acid content in the 'upper SC' in SASP$^{-/-}$ SC implies disruption of several mechanisms for maintenance of SC hydration other than the contribution of NMFs.

As described in the Introduction section, filaggrin is thought to have two major functions: the formation of keratin microfibrils in the lower SC and the production of NMFs in the upper SC (Rawlings & Harding, 2004; Fig 8). It is possible that dry skin of SASP$^{-/-}$ hairless mice is derived from the lower SC where aberrantly processed filaggrin accumulates, but not from the upper SC where the end-products of filaggrin (NMFs) are located. In the normal epidermis of humans, rats and mice, intermediate processing products of mouse filaggrin, 2DI and 3DI, have been reported, and they possess keratin binding activity similar to monomeric filaggrin (Harding & Scott, 1983). Thus, it is suggested that aberrant dimeric and trimeric filaggrins in the SASP$^{-/-}$ SC also possess keratin binding activity. It is widely believed that the SC hydration and physiological and physical mechanics are closely linked and depend on keratin structural organization. Accumulation of premature processed profilaggrin, even if there is keratin binding activity, may alter the cubic-like, rod-packing symmetry of keratin filaments at the SG-to-SC transition and/or at the lower SC, and this may cause alteration of the SC hydration level in the SASP$^{-/-}$ epidermis (Norlen & Al-Amoudi, 2004). The SC of flaky tail mice, in which filaggrin is absent in the cornified cell layers of the epidermis, did not show decreased SC hydration nor an increased number of layers in the SC (Fallon et al, 2009; Presland et al, 2000; Scharschmidt et al, 2009). This suggests that aberrantly processed profilaggrin and a marked decrease of mature filaggrin affect the texture and hydration of the SC. The importance of the amount of mature filaggrin for SC hydration was reported by Ginger et al, who found an inverse relationship between the profilaggrin-12-repeat allele and the occurrence of self-perceived dry skin (Ginger et al, 2005).

SASPase may cleave other as yet unidentified substrates, in addition to profilaggrin, resulting in decreased SC hydration via abnormalities in the intercellular lamellar lipids barrier, the diffusion path length and/or the composition of non-filaggrin-derived NMFs. These possibilities can be examined by crossing SASP$^{-/-}$ mice with filaggrin-deficient mice to examine whether dry skin is derived from aberrant profilaggrin processing.

In normal, healthy controls and AD patients, we identified several missense mutations, which may have affected the activity of SASPase. Among them, we identified a loss-of-function mutation of SASPase (V243A) in non-AD controls. This mutation was located inside the protease domain and no longer showed any activity at pH 6.0. Another missense mutation, V187I, was the most frequently identified in the AD patients (three AD patients). It was located outside of the protease domain at the autoprocessing site, the 'P4' position of the substrate recognition site. A change of the amino acid at P4 resulted in decreased autoprocessing activity *in vitro*. GST-hSASP28(V187I) did not show any autoprocessing activity in *E. coli* (neutral pH), suggesting that this mutation had no activity in the cytoplasm of the SG, resulting in the same loss-of-function effect as SASPase(V243A). SASPase, as a retroviral aspartic protease, must undergo homodimeric formation for its protease activity (Bernard et al, 2005; Matsui et al, 2006). In the HIV protease, a subunit exchange reaction with a catalytically defective protease results in 50% inhibition of enzymatic activity (Darke, 1994). In the case of a heterozygous loss-of-function mutation of bi-allelic expression, half of the molecules are catalytically inactive and induce 'heterodimeric inhibition' of SASPase activity, resulting in a quarter decrease of total activity. The newly found, rare mutations of SASPase (V187I)/(V243A) possibly behave in a dominant negative manner in the person who has the heterozygous mutation.

Of note, the SASP$^{-/-}$ mice showed decreased SC hydration without alteration of TEWL, suggesting a decreased ability of water retention in the SC under normal barrier function. Although the TEWL is an important hallmark for skin barrier function, TEWL is not necessarily correlated with dry skin (Berry et al, 1999; Engelke et al, 1997; Wilhelm et al, 1991). Decreased SC hydration is found in a number of diseases, such as AD, eczema or psoriasis (Harding et al, 2000). There are a number of human epidermal diseases that include the aberrant expression and processing of profilaggrin to filaggrin (reviewed in Dale et al, 1990). Therefore, it is possible that patients who do not have a nonsense mutation of filaggrin, but who exhibit xerosis or AD, might have an aberrant profilaggrin processing pattern. Involvement of SASPase in progression of these diseases from the aspect of the profilaggrin processing pathway should be examined. The profilaggrin degradation pattern could be useful for the diagnosis of xerosis and the early onset of AD.

Collectively, these results indicate that activity of SASPase plays a key role in determining the texture of the SC by modulating SC hydration as well as profilaggrin-to-filaggrin processing. Moreover, these results, in combination with clinicopathological investigations of epidermal diseases derived from the aberrant processing of profilaggrin by SASPase mutation, will provide a novel concept to dissect the complex mechanisms of percutaneous antigen priming in atopic diseases.

The paper explained

PROBLEM:

The SC is the outermost layer of the skin in terrestrial animals and thus acts as a barrier against the external environment. It is hydrated by endogenous substances to avoid desiccation; however, the mechanisms responsible for maintaining hydration of the SC remain unclear at the molecular level. Dry skin is a common phenotype in patients with atopic dermatitis (AD). Recent reports have indicated that the protein filaggrin is mutated in ichthyosis vulgaris patients and is a major predisposing factor for development of atopic eczema, asthma, and allergies. Approximately 50 and 80% of European and Japanese AD patients, respectively, have normal filaggrin alleles, suggesting the presence of previously unidentified predisposing factors.

RESULTS:

We produced 'hairless' mice that were deficient in the enzyme skin-specific retroviral-like aspartic protease (SASPase). The decreased activity of this enzyme in the mice resulted in dry skin with an accumulation of incorrectly processed profilaggrin, a precursor of the filaggrin protein. This incorrectly processed and accumulated profilaggrin subsequently results in a marked decrease of filaggrin production. We also demonstrated that SASPase directly cleaved a profilaggrin linker peptide *in vitro*. Several missense mutations were detected in 5 of 196 AD patients and 2 of 28 normal individuals. Among these, the V243A mutation resulted in complete ablation of protease activity *in vitro*, while the V187I mutation induced a marked decrease in SASPase activity.

IMPACT:

This is the first report demonstrating that a deficiency of the protease SASPase is a likely cause of dry skin *in vivo*. We clarified that the activity of SASPase plays a key role in determining the texture of the SC by modulating SC hydration. This molecular mechanism will provide clues in revealing the role of the SC in terrestrial animals and how they adapted to life on land. Our results also provide novel concepts to assist in determining the complex pathophysiology of atopic dry skin.

MATERIALS AND METHODS

Reagents

Oligonucleotide primers were purchased from Sigma–Aldrich Japan (Kyoto, Japan). N-terminal amino acid sequence analysis was performed by Shimadzu Techno Research (Kyoto, Japan).

Antibodies

For immunofluorescence and immunoblotting, antibodies against keratin 14, keratin 1, involucrin, loricrin and filaggrin were used (Covance, Berkeley, CA). A polyclonal antibody against SASPase, anti-SASP-C, which recognizes the C-terminus of both 28 kDa (human) and 32 kDa (mouse) SASPase, and anti-SASP-PR1 polyclonal antibody, which recognizes both 14 kDa (human) and 15 kDa (mouse) SASPase, have been described previously (Matsui et al, 2006).

Animals

Hairless mice (Hos/HR-1) were obtained from Hoshino Experimental Animal Supply (Ibaragi, Japan). $SASP^{+/-}$ mice of a C57BL/6J background were bred from six generations to a pure Hos/HR-1 background through the speed congenic services of the Central Institute for Experimental Animals (Kawasaki, Japan). Mice heterozygous for a SASPase deletion were interbred, and $SASP^{+/+}$, $SASP^{+/-}$ and $SASP^{-/-}$ littermates were used for experiments. Wild-type (WT, $SASP^{+/+}$), SASPase heterogenic ($SASP^{+/-}$) and SASPase knockout ($SASP^{-/-}$) mice on a Hos/HR-1 backgrounds were used in the study. All mice were maintained under specific pathogen-free (SPF) conditions that are required for maintaining mouse colonies. All animal procedures were approved by the Animal Studies Subcommittee (Institutional Animal Care and Use Committee) of the Tokyo Medical and Dental University and performed in accordance with their guidelines. Basal SC hydration was measured with ASA-M1 (Asahi Biomed, Tokyo, Japan) on the back skin of $SASP^{+/+}$ ($n = 7$) and $SASP^{-/-}$ ($n = 11$) mice. From the same mice, TEWL measurements were taken under basal conditions with a VAVO SCAN (Asahi Biomed). Experiments were performed with adult female mice only (2–5 months old).

Tape-stripped epidermal extract

The dorsal and back skin of $SASP^{+/+}$, $SASP^{+/-}$ and $SASP^{-/-}$ hairless mice were sequentially stripped with Scotch Book Tape 10 times (3M, St. Paul, MN). Corneocytes adherent to the tape surface were eluted by 5 ml of urea-buffer and concentrated by an Amicon-ultra 10 kDa (Millipore) into 50 μl. Protein concentrations were estimated by the Bradford method. Samples were mixed with 25 μl of 3 × SDS sample buffer.

Free amino acid analysis

Surface samples of SC were obtained by adhesive tape striping (Scotch Book Tape) performed five times. Each tape corresponded to a skin area of about $3 \times 10\,cm^2$ derived from anesthetized $SASP^{+/+}$ ($n = 7$) and $SASP^{-/-}$ ($n = 11$) hairless mice. Water-soluble amino acids on the adhesive tapes were extracted with 5 ml 0.1% Triton X-100. After sonication for 30 min at 37 °C, amino acids were quantified using an amino acid analyser (Hitachi model L-8500).

Autoprocessing assay

Fifty microlitres of GST-hSASP28 mutants (1.4 mg/ml or 0.9 mg/ml) in buffer D (50 mM phosphate buffer, pH 6.0, 0.7 M NaCl) containing 1 mM EDTA and protease inhibitor cocktail) was incubated at 37°C. Five-microlitres aliquots were recovered at different times during the

incubation step, and the reaction was stopped by the addition of 20 μl Laemmli buffer. All the aliquots (5 μl) were analysed by SDS-PAGE on 15% acrylamide gels followed by staining with CBB R-250. Semi-quantification of hSASP14 was analysed densitometrically using Adobe Photoshop™ CS3.

Purification of recombinant hSASP14

All procedures were performed at 4°C. Purified GST-hSASP28 was dialysed against buffer D using NAP-10 (GE Healthcare, Japan) and concentrated and frozen at −80 °C. Next, 300 μl of concentrated GST-SASP28 (5 mg/ml) was incubated for 60 min at 37°C to commence autoprocessing. Each sample was diluted in 1 ml of buffer D and passed over 200 μl of Glutathione Sepharose 4B beads (GE Healthcare) twice. The flow-through fraction containing hSASP14 was collected and subjected to the protease assay.

Human filaggrin cleavage assay

Purified hSASP14 (419 pmol) was incubated with 3.6 μM MBP-hFilaggrin in 100 μl of buffer D in the presence of 1 mM EDTA and protease inhibitor cocktail for 60 min at 37°C. After incubation, the reactions were stopped by adding 50 μl of 3 × SDS sample buffer, and 10 μl was subjected to SDS-PAGE. Cleaved fragments were subjected to N-terminal amino acid sequencing.

Author contributions

TM conceived of the study, participated in its design and coordination, carried out the analysis of knockout mice and the biochemical studies and drafted the manuscript; KM and JK carried out the mutation search; AK participated in the design of the study and helped to draft the manuscript; HK and TE conducted the human study; KH and ST helped to analyse the knockout mice; SI carried out the electron microscopic analysis; II and JI participated in the design and coordination of the study and helped to draft the manuscript; MA conceived of the study, participated in its design and coordination and helped to draft the manuscript. All authors read and approved the final manuscript.

Acknowledgements

We thank Sayaka Katahira-Tayama and Itsumi Ohmori for technical assistance. We thank Dr. Tsuyohi Hata (KOSÉ Corporation) for helpful discussions. We thank KAN Research Institute Inc. for providing materials. This work was supported by a Grant-in-Aid for Scientific Research to TM to AK, and to HK, 'Program for Improvement of Research Environment for Young Researchers' from the Ministry of Education, Culture, Sports, Science and Technology (MEXT) of Japan to TM and to AK, research grants from the Nakatomi Foundation, the Cosmetology Research Foundation and the Naito Foundation to TM, the Keio University Global Center of Excellence Program for In vivo Human Metabolomic Systems Biology from MEXT and Health and Labour Sciences Research Grants for Research on Allergic Diseases and Immunology from the Ministry of Health, Labour and Welfare.

Supporting information is available at EMBO Molecular Medicine online.

The authors declare that they have no conflicts of interest.

For more information

OMIM: SKIN ASPARTIC PROTEASE:
http://www.ncbi.nlm.nih.gov/omim/611765

GeneCards:
http://www.genecards.org/cgi-bin/carddisp.pl?gene=ASPRV1

References

Barker JN, Palmer CN, Zhao Y, Liao H, Hull PR, Lee SP, Allen MH, Meggitt SJ, Reynolds NJ, Trembath RC *et al* (2007) Null mutations in the filaggrin gene (FLG) determine major susceptibility to early-onset atopic dermatitis that persists into adulthood. J Invest Dermatol 127: 564-567

Barnes KC (2010) An update on the genetics of atopic dermatitis: scratching the surface in 2009. J Allergy Clin Immunol 125: 16-29 e11–11; quiz 30-11

Bernard D, Mehul B, Thomas-Collignon A, Delattre C, Donovan M, Schmidt R (2005) Identification and characterization of a novel retroviral-like aspartic protease specifically expressed in human epidermis. J Invest Dermatol 125: 278-287

Berry N, Charmeil C, Goujon C, Silvy A, Girard P, Corcuff P, Montastier C (1999) A clinical, biometrological and ultrastructural study of xerotic skin. Int J Cosmet Sci 21: 241-252

Candi E, Tarcsa E, Digiovanna JJ, Compton JG, Elias PM, Marekov LN, Steinert PM (1998) A highly conserved lysine residue on the head domain of type II keratins is essential for the attachment of keratin intermediate filaments to the cornified cell envelope through isopeptide crosslinking by transglutaminases. Proc Natl Acad Sci USA 95: 2067-2072

Candi E, Schmidt R, Melino G (2005) The cornified envelope: a model of cell death in the skin. Nat Rev Mol Cell Biol 6: 328-340

Dale BA, Holbrook KA, Steinert PM (1978) Assembly of stratum corneum basic protein and keratin filaments in macrofibrils. Nature 276: 729-731

Dale BA, Resing KA, Lonsdale-Eccles JD (1985) Filaggrin: a keratin filament associated protein. Ann NY Acad Sci 455: 330-342

Dale BA, Resing KA, Haydock PV (1990) Filaggrins. In: *Cellular and Molecular Biology of Intermediate Filaments*, Goldman RD and Steinert PM, (eds), New York and London, Plenum Press: pp 393-412.

Darke PL (1994) Stability of dimeric retroviral proteases. Methods Enzymol 241: 104-127

Denecker G, Hoste E, Gilbert B, Hochepied T, Ovaere P, Lippens S, Van den Broecke C, Van Damme P, D'Herde K, Hachem JP *et al* (2007) Caspase-14 protects against epidermal UVB photodamage and water loss. Nat Cell Biol 9: 666-674

Elias PM, Steinhoff M (2008) "Outside-to-inside" (and now back to "outside") pathogenic mechanisms in atopic dermatitis. J Invest Dermatol 128: 1067-1070

Engelke M, Jensen JM, Ekanayake-Mudiyanselage S, Proksch E (1997) Effects of xerosis and ageing on epidermal proliferation and differentiation. Br J Dermatol 137: 219-225

Fallon PG, Sasaki T, Sandilands A, Campbell LE, Saunders SP, Mangan NE, Callanan JJ, Kawasaki H, Shiohama A, Kubo A *et al* (2009) A homozygous frameshift mutation in the mouse Flg gene facilitates enhanced percutaneous allergen priming. Nat Genet 41: 602-608

Fluhr JW, Darlenski R, Surber C (2008) Glycerol and the skin: holistic approach to its origin and functions. Br J Dermatol 159: 23-34

Ginger RS, Blachford S, Rowland J, Rowson M, Harding CR (2005) Filaggrin repeat number polymorphism is associated with a dry skin phenotype. Arch Dermatol Res 297: 235-241

Harding CR, Scott IR (1983) Histidine-rich proteins (filaggrins): structural and functional heterogeneity during epidermal differentiation. J Mol Biol 170: 651-673

Harding CR, Watkinson A, Rawlings AV, Scott IR (2000) Dry skin, moisturization and corneodesmolysis. Int J Cosmet Sci 22: 21-52

Hildenbrand M, Rhiemeier V, Hartenstein B, Lahrmann B, Grabe N, Angel P, Hess J (2010) Impaired skin regeneration and remodeling after cutaneous injury and chemically induced hyperplasia in taps-transgenic mice. J Invest Dermatol 130: 1922-1930

Irvine AD (2007) Fleshing out filaggrin phenotypes. J Invest Dermatol 127: 504-507

Ishida-Yamamoto A, Senshu T, Eady RA, Takahashi H, Shimizu H, Akiyama M, Iizuka H (2002) Sequential reorganization of cornified cell keratin filaments involving filaggrin-mediated compaction and keratin 1 deimination. J Invest Dermatol 118: 282-287

Kamata Y, Taniguchi A, Yamamoto M, Nomura J, Ishihara K, Takahara H, Hibino T, Takeda A (2009) Neutral cysteine protease bleomycin hydrolase is essential for the breakdown of deiminated filaggrin into amino acids. J Biol Chem 284: 12829-12836

Leyvraz C, Charles RP, Rubera I, Guitard M, Rotman S, Breiden B, Sandhoff K, Hummler E (2005) The epidermal barrier function is dependent on the serine protease CAP1/Prss8. J Cell Biol 170: 487-496

List K, Szabo R, Wertz PW, Segre J, Haudenschild CC, Kim SY, Bugge TH (2003) Loss of proteolytically processed filaggrin caused by epidermal deletion of Matriptase/MT-SP1. J Cell Biol 163: 901-910

Matsui T, Hayashi-Kisumi F, Kinoshita Y, Katahira S, Morita K, Miyachi Y, Ono Y, Imai T, Tanigawa Y, Komiya T *et al* (2004) Identification of novel keratinocyte-secreted peptides dermokine-alpha/-beta and a new stratified epithelium-secreted protein gene complex on human chromosome 19q13.1. Genomics 84: 384-397

Matsui T, Kinoshita-Ida Y, Hayashi-Kisumi F, Hata M, Matsubara K, Chiba M, Katahira-Tayama S, Morita K, Miyachi Y, Tsukita S (2006) Mouse homologue of skin-specific retroviral-like aspartic protease involved in wrinkle formation. J Biol Chem 281: 27512-27525

McGrath JA, Uitto J (2008) The filaggrin story: novel insights into skin-barrier function and disease. Trends Mol Med 14: 20-27

Mechin MC, Enji M, Nachat R, Chavanas S, Charveron M, Ishida-Yamamoto A, Serre G, Takahara H, Simon M (2005) The peptidylarginine deiminases expressed in human epidermis differ in their substrate specificities and subcellular locations. Cell Mol Life Sci 62: 1984-1995

Nachat R, Mechin MC, Takahara H, Chavanas S, Charveron M, Serre G, Simon M (2005) Peptidylarginine deiminase isoforms 1–3 are expressed in the epidermis and involved in the deimination of K1 and filaggrin. J Invest Dermatol 124: 384-393

Nomura T, Akiyama M, Sandilands A, Nemoto-Hasebe I, Sakai K, Nagasaki A, Ota M, Hata H, Evans AT, Palmer CN *et al* (2008) Specific filaggrin mutations cause ichthyosis vulgaris and are significantly associated with atopic dermatitis in Japan. J Invest Dermatol 128: 1436-1441

Norlen L, Al-Amoudi A (2004) Stratum corneum keratin structure, function, and formation: the cubic rod-packing and membrane templating model. J Invest Dermatol 123: 715-732

Palmer CN, Irvine AD, Terron-Kwiatkowski A, Zhao Y, Liao H, Lee SP, Goudie DR, Sandilands A, Campbell LE, Smith FJ *et al* (2006) Common loss-of-function variants of the epidermal barrier protein filaggrin are a major predisposing factor for atopic dermatitis. Nat Genet 38: 441-446

Pearton DJ, Nirunsuksiri W, Rehemtulla A, Lewis SP, Presland RB, Dale BA (2001) Proprotein convertase expression and localization in epidermis: evidence for multiple roles and substrates. Exp Dermatol 10: 193-203

Presland RB, Boggess D, Lewis SP, Hull C, Fleckman P, Sundberg JP (2000) Loss of normal profilaggrin and filaggrin in flaky tail (ft/ft) mice: an animal model for the filaggrin-deficient skin disease ichthyosis vulgaris. J Invest Dermatol 115: 1072-1081

Presland RB, Rothnagel JA, Lawrence OT (2006) Profilaggrin and the fused S100 family of calcium-binding proteins. In: *In Skin Barrier*, Elias PM and Feingold KR, (eds) New York, Taylor and Francis: pp 111-140.

Rawlings AV, Harding CR (2004) Moisturization and skin barrier function. Dermatol Ther 17: 43-48

Rawlings AV, Matts PJ (2005) Stratum corneum moisturization at the molecular level: an update in relation to the dry skin cycle. J Invest Dermatol 124: 1099-1110

Resing KA, Walsh KA, Haugen-Scofield J, Dale BA (1989) Identification of proteolytic cleavage sites in the conversion of profilaggrin to filaggrin in mammalian epidermis. J Biol Chem 264: 1837-1845

Resing KA, al-Alawi N, Blomquist C, Fleckman P, Dale BA (1993) Independent regulation of two cytoplasmic processing stages of the intermediate filament-associated protein filaggrin and role of Ca^{2+} in the second stage. J Biol Chem 268: 25139-25145

Resing KA, Johnson RS, Walsh KA (1993) Characterization of protease processing sites during conversion of rat profilaggrin to filaggrin. Biochemistry 32: 10036-10045

Resing KA, Thulin C, Whiting K, al-Alawi N, Mostad S (1995) Characterization of profilaggrin endoproteinase 1. A regulated cytoplasmic endoproteinase of epidermis. J Biol Chem 270: 28193-28198

Rhiemeier V, Breitenbach U, Richter KH, Gebhardt C, Vogt I, Hartenstein B, Furstenberger G, Mauch C, Hess J, Angel P (2006) A novel aspartic proteinase-like gene expressed in stratified epithelia and squamous cell carcinoma of the skin. Am J Pathol 168: 1354-1364

Sandilands A, Terron-Kwiatkowski A, Hull PR, O'Regan GM, Clayton TH, Watson RM, Carrick T, Evans AT, Liao H, Zhao Y *et al* (2007) Comprehensive analysis of the gene encoding filaggrin uncovers prevalent and rare mutations in ichthyosis vulgaris and atopic eczema. Nat Genet 39: 650-654

Sandilands A, Sutherland C, Irvine AD, McLean WH (2009) Filaggrin in the frontline: role in skin barrier function and disease. J Cell Sci 122: 1285-1294

Sasaki T, Kudoh J, Ebihara T, Shiohama A, Asakawa S, Shimizu A, Takayanagi A, Dekio I, Sadahira C, Amagai M *et al* (2008) Sequence analysis of filaggrin gene by novel shotgun method in Japanese atopic dermatitis. J Dermatol Sci 51: 113-120

Scharschmidt TC, Man MQ, Hatano Y, Crumrine D, Gunathilake R, Sundberg JP, Silva KA, Mauro TM, Hupe M, Cho S *et al* (2009) Filaggrin deficiency confers a paracellular barrier abnormality that reduces inflammatory thresholds to irritants and haptens. J Allergy Clin Immunol 124: 496-506, 506 e491-496

Smith FJ, Irvine AD, Terron-Kwiatkowski A, Sandilands A, Campbell LE, Zhao Y, Liao H, Evans AT, Goudie DR, Lewis-Jones S *et al* (2006) Loss-of-function mutations in the gene encoding filaggrin cause ichthyosis vulgaris. Nat Genet 38: 337-342

Steinert PM, Marekov LN (1995) The proteins elafin, filaggrin, keratin intermediate filaments, loricrin, and small proline-rich proteins 1 and 2 are isodipeptide cross-linked components of the human epidermal cornified cell envelope. J Biol Chem 270: 17702-17711

Tarcsa E, Marekov LN, Mei G, Melino G, Lee SC, Steinert PM (1996) Protein unfolding by peptidylarginine deiminase. Substrate specificity and structural relationships of the natural substrates trichohyalin and filaggrin. J Biol Chem 271: 30709-30716

Thulin CD, Walsh KA (1995) Identification of the amino terminus of human filaggrin using differential LC/MS techniques: implications for profilaggrin processing. Biochemistry 34: 8687-8692

Thulin CD, Taylor JA, Walsh KA (1996) Microheterogeneity of human filaggrin: analysis of a complex peptide mixture using mass spectrometry. Protein Sci 5: 1157-1164

Wakeland E, Morel L, Achey K, Yui M, Longmate J (1997) Speed congenics: a classic technique in the fast lane (relatively speaking). Immunol Today 18: 472-477

Watt FM (1989) Terminal differentiation of epidermal keratinocytes. Curr Opin Cell Biol 1: 1107-1115

Wilhelm KP, Cua AB, Maibach HI (1991) Skin aging. Effect on transepidermal water loss, stratum corneum hydration, skin surface pH, and casual sebum content. Arch Dermatol 127: 1806-1809

Yamazaki M, Ishidoh K, Suga Y, Saido TC, Kawashima S, Suzuki K, Kominami E, Ogawa H (1997) Cytoplasmic processing of human profilaggrin by active mu-calpain. Biochem Biophys Res Commun 235: 652-656

Published December 5, 2011

JEM

Brief Definitive Report

Langerhans cell antigen capture through tight junctions confers preemptive immunity in experimental staphylococcal scalded skin syndrome

Takeshi Ouchi,[1] Akiharu Kubo,[1,2] Mariko Yokouchi,[1,2] Takeya Adachi,[1,2] Tetsuro Kobayashi,[1] Daniela Y. Kitashima,[1,2] Hideki Fujii,[3] Björn E. Clausen,[4] Shigeo Koyasu,[3] Masayuki Amagai,[1] and Keisuke Nagao[1]

[1]Department of Dermatology, [2]Center for Integrated Medical Research, and [3]Department of Microbiology and Immunology, Keio University School of Medicine, Shinjuku-ku, Tokyo 160-8582, Japan
[4]Department of Immunology, Erasmus University Medical Center, 3015 CE Rotterdam, Netherlands

Epidermal Langerhans cells (LCs) extend dendrites through tight junctions (TJs) to survey the skin surface, but their immunological contribution in vivo remains elusive. We show that LCs were essential for inducing IgG_1 responses to patch-immunized ovalbumin in mice that lacked skin dendritic cell subsets. The significance of LC-induced humoral responses was demonstrated in a mouse model of staphylococcal scalded skin syndrome (SSSS), a severe blistering disease in which the desmosomal protein Dsg1 (desmoglein1) is cleaved by *Staphylococcus aureus*–derived exfoliative toxin (ET). Importantly, ET did not penetrate TJs, and patch immunization did not alter epidermal integrity. Nevertheless, neutralizing anti-ET IgG_1 was induced after patch immunization and abolished upon LC depletion, indicating that antigen capture through TJs by LCs induced humoral immunity. Strikingly, the ET-patched mice were protected from developing SSSS after intraperitoneal ET challenge, whereas LC-depleted mice were susceptible to SSSS, demonstrating a vital role for LC-induced IgG_1 in systemic defense against circulating toxin in vivo. Therefore, LCs elicit humoral immunity to antigens that have not yet violated the epidermal barrier, providing preemptive immunity against potentially pathogenic skin microbes. Targeting this immunological process confers protection with minimal invasiveness and should have a marked impact on future strategies for development of percutaneous vaccines.

CORRESPONDENCE
Keisuke Nagao:
nagaok@z8.keio.jp

Abbreviations used: ACT, antigen capture through TJs; dDC, dermal DC; DT, diphtheria toxin; DTR, DT receptor; ET, exfoliative toxin; hrDsg1, human recombinant Dsg1; LC, Langerhans cell; SSSS, staphylococcal scalded skin syndrome; TJ, tight junction.

The longstanding Langerhans cell (LC) paradigm (Schuler and Steinman, 1985; Wilson and Villadangos, 2004) holds that LCs acquire skin-associated antigens and present them to T cells upon migrating to skin-draining lymph nodes. However, a series of recent studies using transgenic mouse models has failed to clearly demonstrate a critical contribution of LCs in the induction of immunity to percutaneous antigens in vivo.

LCs were dispensable for antiviral immunity in a herpes simplex virus skin scarification model (Allan et al., 2003), and mouse models in which LCs were transiently or constitutively depleted showed that they were not essential for eliciting hapten-induced contact hypersensitivity (Kaplan et al., 2005; Kissenpfennig et al., 2005; Bennett et al., 2007). It is possible that LCs are tolerogenic, but this may depend on the nature of the antigen (e.g., foreign or self), route of antigen exposure (e.g., through the epidermis or directly into the dermis), and presence or absence of environmental cues, including interactions with pathogens (Kautz-Neu et al., 2011).

We recently reported that LCs induced IgG_1 (Th2) responses to gene gun–immunized bacterial antigens and that skin DC subsets had distinct roles in inducing humoral responses (Nagao et al., 2009). Although this experimental

The Rockefeller University Press $30.00
J. Exp. Med. Vol. 208 No. 13 2607-2613
www.jem.org/cgi/doi/10.1084/jem.20111718

Supplemental Material can be found at:
http://jem.rupress.org/content/suppl/2011/12/01/jem.20111718.DC1.html

Published December 5, 2011

procedure represented in vivo data with antigen specificity, it circumvented the epidermal barrier system and antigen uptake processes. Our subsequent study demonstrated that LCs extend dendrites through the tight junctions (TJs) to the stratum corneum and capture protein antigens without disturbing barrier integrity (Kubo et al., 2009). These findings indicate that LCs survey not only within the skin but also on the skin surface outside of the TJs. In this study, we focused on antigen capture through TJs (ACT) by LCs to determine whether these enigmatic skin DCs are capable of inducing immune responses to percutaneous protein antigens. We used a model of experimental staphylococcal scalded skin syndrome (SSSS), a severe blistering disease caused by exfoliative toxin (ET)–producing *Staphylococcus aureus* (Stanley and Amagai, 2006), to further demonstrate the critical role of LCs in protective immunity in vivo.

RESULTS AND DISCUSSION

To test whether ACT by LCs leads to antigen-specific IgG_1 responses against protein antigens, we patch-immunized WT C57BL/6 mice with OVA three times at 5-d intervals and determined serum anti-OVA antibody levels by ELISA (Fig. 1 A). TJs regulate paracellular trafficking of ions and do not allow passage of soluble proteins (Vermeer et al., 2003). Therefore, OVA

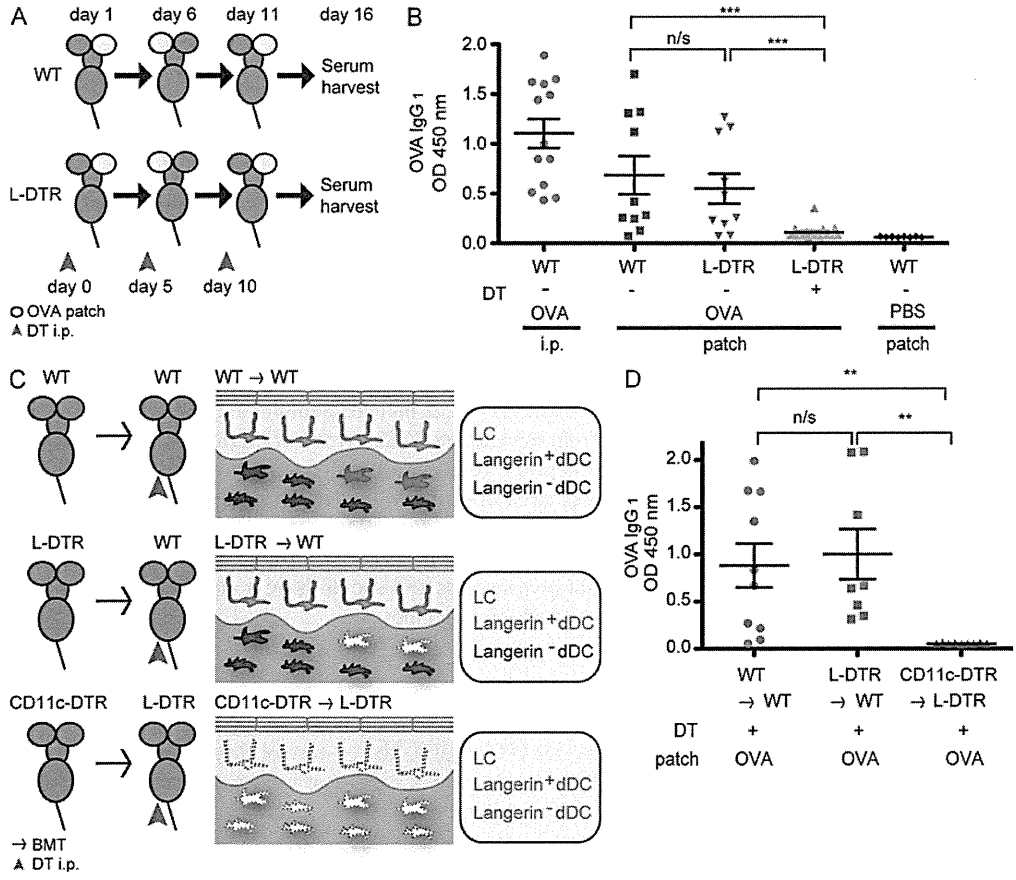

Figure 1. LCs are essential for the induction of IgG_1 responses to OVA captured through TJs. (A) Patch immunization protocol. 4 mg/ml OVA in PBS was used to patch immunize mice via an occlusive dressing on the gently tape-stripped ears (yellow); the patch was removed after 24 h. In DC depletion experiments, DT was administered i.p. to mice 24 h before each patch immunization. (B) OVA-specific IgG_1 responses were determined by ELISA of sera (1:500 dilution) from mice that received OVA i.p. (n = 13), OVA-patched WT mice (n = 10), Langerin-DTR mice without DT i.p. (n = 10), Langerin-DTR mice with DT i.p. (n = 17), and PBS-patched (n = 8) WT mice. ***, P = 0.0006 (second lane vs. fourth lane) and P = 0.0008 (third lane vs. fourth lane) by Student's t test. Shown are results from a single experiment representative of three experiments. (C) Lethally irradiated recipient mice were reconstituted with BM from the indicated donor mice. After complete chimerism, the mice were treated with DT i.p. to generate mice that harbored (top; WT → WT) or lacked (bottom; CD11c-DTR → L-DTR) all skin DCs and mice that lacked only langerin$^+$ dDCs (middle; L-DTR → WT). BMT, BM transfer. (D) OVA-specific IgG_1 responses in sera (1:500 dilution) of mice from C. n = 10 WT → WT, n = 8 L-DTR → WT, and n = 9 CD11c-DTR → L-DTR mice from a single experiment that was reproduced in a similar, independent experiment. **, P = 0.0035 (first lane vs. third lane) and P = 0.0017 (second lane vs. third lane) by Student's t test. (B and D) Error bars represent mean value ± SEM.

Published December 5, 2011

does not pass through TJs but can be taken up by LCs across the TJ barrier, as we have recently shown (Kubo et al., 2009).

Consistent with our previous results using gene gun immunization (Nagao et al., 2009), WT mice produced OVA-specific antibodies restricted to the IgG_1 subclass (Fig. 1 B). To determine the contribution of LCs, we used Langerin-DTR (diphtheria toxin [DT] receptor) mice (Bennett et al., 2005), in which langerin-expressing cells are selectively and transiently depleted upon DT treatment. Langerin$^+$ dermal DCs (dDCs), a recently described dDC subset (Bursch et al., 2007; Ginhoux et al., 2007; Poulin et al., 2007), do not repopulate the dermis for 3–7 d, and LCs do not repopulate the epidermis for at least 2 wk during steady-state after conditional depletion (Nagao et al., 2009; Noordegraaf et al., 2010). Langerin-DTR mice received i.p. DT 1 d before each patch immunization (Fig. 1 A). In contrast to the robust IgG_1 responses obtained in WT and DT-untreated Langerin-DTR mice, the responses were abolished in DT-treated Langerin-DTR mice, demonstrating that langerin-expressing DCs were required for humoral responses to patch-immunized protein antigens (Fig. 1 B).

Given that langerin$^+$ dDCs are also depleted in this experimental setting (Nagao et al., 2009), we combined conditional depletion and BM transplantation to generate mice in which only langerin$^+$ dDCs (Langerin-DTR BM → WT) or all DCs (CD11c-DTR BM → Langerin-DTR) were depleted, as well as mice that harbored all DCs (WT BM → WT; Fig. 1 C and Fig. S1). As LCs are radio resistant (Merad et al., 2002), lethally irradiated WT mice chimerized with Langerin-DTR BM could be depleted of langerin$^+$ dDCs upon DT treatment, whereas the LCs of host origin remained unaffected in the epidermis.

Robust anti-OVA responses were observed in mice that harbored all DCs, in contrast to mice that lacked all DCs (Fig. 1 D). Of note, mice that lacked langerin$^+$ dDCs responded with anti-OVA IgG_1 levels similar to those of mice harboring all DCs (Fig. 1 D). These results demonstrate an essential role for LCs but not dDCs in inducing antigen-specific IgG_1 responses subsequent to ACT.

The aforementioned results led us to wonder whether LCs performed ACT to survey for antigens from bacterial flora that could exert pathogenicity under certain conditions. *S. aureus* is a clinically relevant bacterium that is capable of colonizing and/or infecting skin, and SSSS is a severe blistering disease that occurs during childhood, caused by skin infection with *S. aureus* that produces ET (Stanley and Amagai, 2006). ET circulates systemically via the bloodstream to distal skin sites (Nishioka et al., 1977b; Ladhani et al., 1999), where it cleaves Dsg1 (desmoglein1), a desmosomal adhesion molecule of the cadherin family

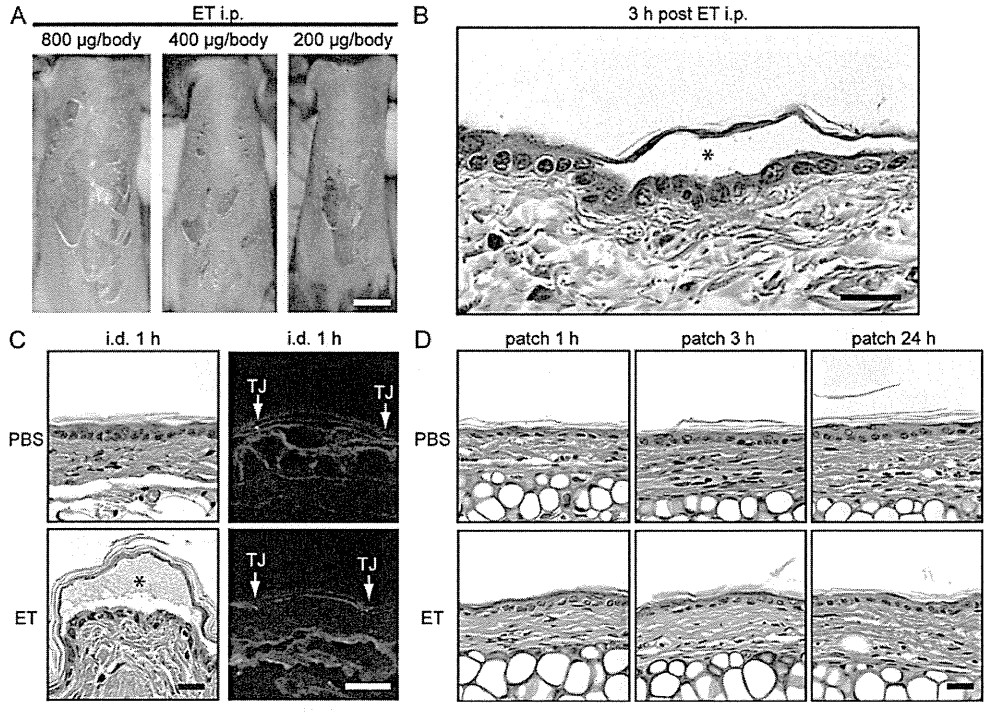

Figure 2. Patch-immunized ETA does not alter epidermal integrity. (A) Development of SSSS 3 h after i.p. injection of ETA. (B) Histological features of superficial acantholysis in experimental SSSS. The asterisk denotes blister formation. (C) Visualization of Dsg1 and TJs in ear skin after intradermal (i.d.) injection of PBS or ETA. Dsg1 (red) and TJs (shown via ZO-1 staining in green; arrows) were visualized in the periphery of the blister in ear skin denoted by the asterisk (bottom) that received ETA intradermally (right). (D) Histological features of ear skin that received PBS or ETA patch immunization for 1, 3, or 24 h (right). Each experiment was performed three times with $n = 3$. Bars: (A) 1 cm; (B, C [left], and D) 25 µm; (C, right) 10 µm.

Published December 5, 2011

which is critical for maintaining cell–cell adhesion in the upper epidermis (Amagai et al., 2000; Stanley and Amagai, 2006).

Anti-ET antibodies can be detected in healthy individuals with no history of SSSS (Yamasaki et al., 2005), and it has been suggested that the presence or absence of circulating anti-ET antibodies may affect disease severity (Nishioka et al., 1977b; Ladhani et al., 1999). Therefore, we sought to determine whether LCs were capable of capturing *S. aureus*–derived ET through intact TJs and subsequently prepare a repertoire of antibodies that conferred protection from SSSS development.

We modified a mouse model of experimental SSSS (Nishioka et al., 1977a) by using recombinant ETA, which is a major isoform of ET along with ETB, in adult mice. A single i.p. injection of ETA induced skin erosions with dose-dependent severity as soon as 3 h after treatment (Fig. 2 A). Epidermal detachment in the granular layer, identical to that seen in human SSSS, was confirmed by histology (Fig. 2 B; Amagai et al., 2000; Stanley and Amagai, 2006). We then determined that TJs do not allow penetration of ETA. When ETA was injected into the dermis, it cleaved Dsg1 on keratinocytes located below but not above the TJ barrier (as visualized by ZO-1; Fig. 2 C). Moreover, tape-stripped skin to which ETA was patch immunized for 1, 3, or 24 h remained intact, with no clinical or histological sign of acantholysis (Fig. 2 D). These findings showed that ETA did not penetrate the epidermal barrier system to reach the viable layers, further suggesting that any immune responses achieved after ETA patch immunization are likely attributable to ACT by LCs.

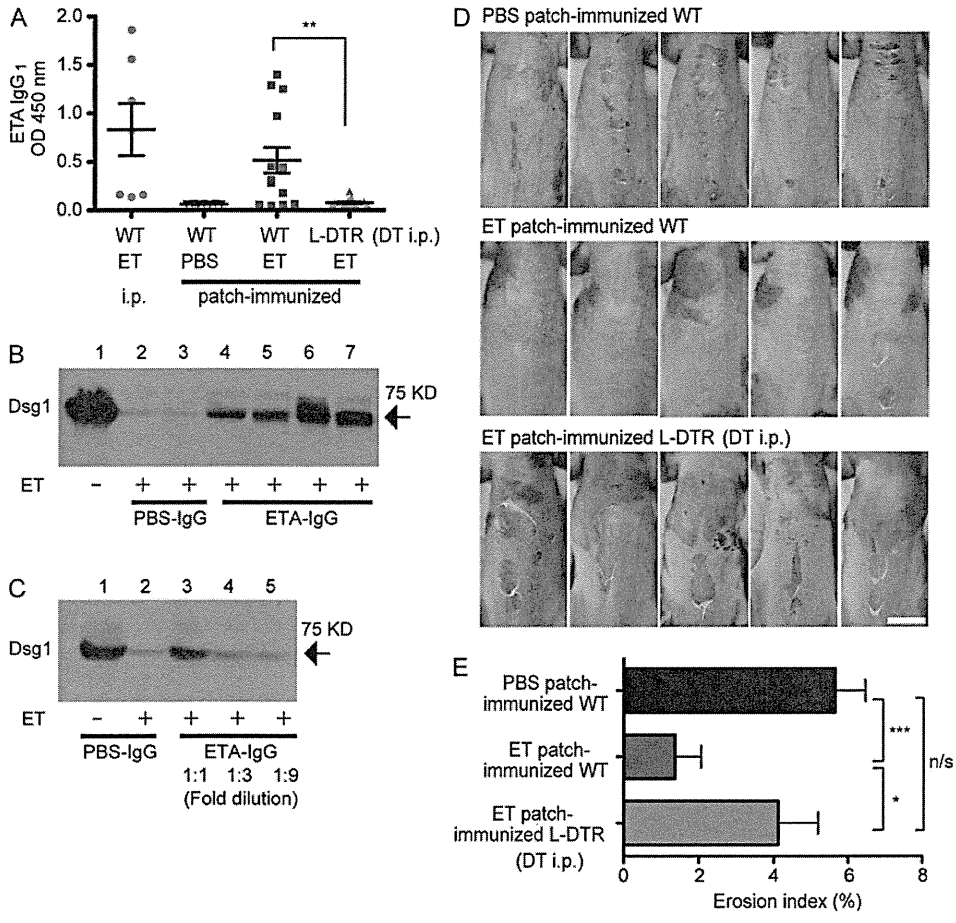

Figure 3. ACT by LCs confers protective and systemic humoral immunity against experimental SSSS. (A) The anti-ETA IgG_1 response in WT mice that received ETA i.p., PBS patch, or ETA patch, as well as Langerin-DTR mice that were treated with DT 1 d before each ETA patch immunization. Sera were diluted 1:500. **, P = 0.0024. (B) Cleavage analysis of hrDsg1. ETA was preincubated with purified IgG from mice patch immunized with either PBS (PBS-IgG) or ETA (ETA-IgG) and then further incubated with hrDsg1. Each lane represents IgG purified from a single mouse. The arrow denotes hrDsg1, ~75 kD in size. (C) Dose dependency of the neutralizing activity of ETA-IgG. (D) PBS patch-immunized WT mice (n = 16), ETA patch-immunized WT mice (n = 14), and DT-treated, ETA patch-immunized Langerin-DTR mice (n = 15) from A were challenged i.p. with 200 µg ETA, and images were taken 3 h later. Shown are representative data from a single experiment. Bar, 1 cm. Experiments in A–C were performed in two other independent experiments and D in one other experiment with similar results. (E) Erosion area index of ventral trunk skin in mice from D. *, P = 0.0432; ***, P = 0.0003. (A and E) Error bars represent mean value ± SEM.

Published December 5, 2011

Consistent with the data in Fig. 1, patch immunization with ETA led to anti-ETA IgG_1 production (Fig. 3 A). Immunization with OVA i.p. resulted predominantly in IgG_1 production, whereas immunization with ETA i.p. induced robust IgG_1, IgG_{2b}, and IgG_{2c} responses, in contrast to the IgG_1-restricted responses induced by ETA patch immunization (Fig. 3 A and Fig. S2). This further supports a role for LCs in driving the Th2 response (Nagao et al., 2009). Importantly, Langerin-DTR mice that were DT treated before each patch immunization failed to mount ETA-specific IgG_1 responses (Fig. 3 A).

To functionally characterize LC-induced anti-ETA IgG_1, we purified IgG from PBS (PBS-IgG) or ETA (ETA-IgG) patch-immunized mice and determined its effect on the Dsg1-cleaving activity of ETA in vitro. Incubation of soluble human recombinant Dsg1 (hrDsg1) with ETA leads to efficient cleavage in vitro (Amagai et al., 2000). Although preincubation of PBS-IgG with ETA had no effect on hrDsg1 cleavage by ETA, the coincubation of ETA-IgG and ETA resulted in a marked decrease in the amount of cleaved hrDsg1 (Fig. 3 B), in a dose-dependent manner (Fig. 3 C), demonstrating that ETA-IgG exerts neutralizing activity toward ETA.

Finally, to directly demonstrate the in vivo role of LC-induced IgG_1, we challenged patch-immunized mice with a single i.p. injection of ETA (200 μg/body). The PBS-immunized mice developed skin erosions (Fig. 3 D, top), but the majority of ETA patch-immunized mice were protected from developing SSSS (Fig. 3 D, middle). In stark contrast, Langerin-DTR mice treated with DT before each immunization developed SSSS (Fig. 3 D, bottom), with skin erosion indices significantly higher than those of ETA patch-immunized mice (Fig. 3 E). These results established the essential role of LCs in the induction of humoral responses that conferred systemic protection against circulating toxin in this model of SSSS.

Collectively, ACT by LCs led to the induction of humoral immunity against ETA in the presence of an intact TJ barrier, and this immunity protected mice from developing experimental SSSS upon systemic ETA challenge. This study reveals a novel preemptive role for LCs in protective humoral immunity in vivo against bacteria-derived pathogenic components that exist on the skin surface but have not yet breached the epidermal barrier. The protein antigens used in this study do not reach the viable epidermal layers, and how B cells in the draining lymph nodes recognize them is an interesting question to be clarified in future studies.

Vaccine development to date has focused on overcoming the epidermal barrier, using a variety of physical forces such as a gene gun and microneedles (Prausnitz et al., 2009; Yager et al., 2009). The current work shows that this may not be essential. Targeting ACT by LCs can be extended to other toxins or pathogens and should have a marked impact on the strategies by which topical vaccines are designed to achieve defined systemic humoral immunity, with minimal invasiveness and stress.

MATERIALS AND METHODS

Mice. Mice were bred in specific pathogen–free facilities at the Keio University School of Medicine. C57BL/6J mice (CLEA), 6–8 wk old, were used for immunization experiments. Heterozygous C57BL/6J Langerin-DTR mice were obtained by breeding homozygous Langerin-DTR mice with C57BL/6J WT mice. CD11c-DTR mice were a gift from D.R. Littman (New York University School of Medicine, New York, NY). All animal procedures and study protocols were approved by the Keio University Ethics Committee for Animal Experiments.

Genomic PCR of Langerin-DTR mice. The *langerin* WT allele was detected using the primers LangWTf1 (5′-TGCTTCTGCCCACAACTGCTCTT-3′) and LangWTb1 (5′-GACACCAAGGACTGTAGCCAAAAGG-3′). The *langerin-DTR* allele was detected by using LangWTf1 and LangDTR2 (5′-TCAGTGGGAATTAGTCATGCC-3′).

In vivo depletion of langerin$^+$ DCs. For in vivo depletion of langerin$^+$ DCs, heterozygous Langerin-DTR mice were injected i.p. with 500 ng DT (Sigma-Aldrich) in sterile PBS.

Patch immunization. The dorsal mouse ears were gently tape-stripped five times with Scotch tape (3M), and double-layered filter paper wetted with 50 μl of 4 mg/ml OVA or ETA in PBS was used to patch immunize the mice, using a patch device (Finn Chamber; SmartPractice). The mice were fitted with plastic collars to avoid scratching of the immunization sites. The Finn Chambers were removed after 24 h, but the collars were kept on for 2 or 3 d to prevent the mice scratching their ears. Immunization was performed three times at 5-d intervals, and the ear that received patch immunization was switched each time from right to left or vice versa to prevent any inadvertent damage to the immunization site. Sera were collected 5 d after the final immunization.

ELISA. The wells of MaxiSorp ELISA plates (Thermo Fisher Scientific) were coated with OVA or ET (50 ng/well) at 4°C overnight. After blocking, sera were serially diluted 1:500 in PBS containing 3% skim milk and added to the wells. The plates were incubated for 2 h at room temperature. After washing, the plates were incubated with horseradish peroxidase–conjugated goat anti–mouse $IgG_{1/2b/2c/3}$ antibodies (Bethyl Laboratories, Inc.) for 2 h. Immunoreactivity was detected with TMB substrate solution (MBL), and enzymatic reactions were halted with 1 M NH_2SO_4 before measuring the optical density at 450 nm.

Generation of BM chimeric mice. 8-wk-old recipient C57BL/6 and/or Langerin-DTR mice were lethally irradiated (9.5 Gy) and reconstituted with 2×10^6 BM cells from C57BL/6, Langerin-DTR, or CD11c-DTR mice.

Antibodies. Rat anti–mouse EpCAM mAb (clone G8.8; Developmental Studies Hybridoma Bank) labeled with Alexa Fluor 568 (Invitrogen), rat anti–mouse langerin mAb (clone L31; provided by C.-G. Park and R. Steinman, The Rockefeller University, New York, NY) labeled with Alexa Fluor 647 (Invitrogen), and FITC-conjugated rat anti–mouse I-A/I-E mAb (clone M5/114.15.2; BioLegend) for detection of MHC class II were used for immunohistochemistry of epidermal and dermal sheets. Anti–mouse CD16/32 mAb (clone 93; BioLegend) was routinely used to block Fc receptors before staining, and cell nuclei were stained with Hoechst 33258 (Invitrogen). Mouse anti–ZO-1 mAb (clone T8-754 [Itoh et al., 1991]; provided by M. Furuse, Kobe University, Kobe, Japan), anti-Dsg1 scFVs mAb with a hemagglutinin tag (provided by K. Ishii, Teikyo University Chiba Medical Center, Ichihara, Japan; Ishii et al., 2008), and an antihemagglutinin mAb were used for cryosection staining (3F10; Roche). Goat anti–E tag polyclonal antibody (Abcam) and horseradish peroxidase–conjugated donkey anti–goat IgG polyclonal antibody were used for immunoblotting.

Preparation and staining of epidermal and dermal sheets and cryosections. Epidermal and dermal sheets were prepared with 3.8% ammonium thiocyanate (Wako) in 100 mM sodium phosphate (Nagao et al., 2009). Sheets were fixed in cold acetone and blocked with 3% skim milk (Morinaga), anti-CD16/32 mAb, and goat serum (Jackson ImmunoResearch Laboratories, Inc.) in PBS before incubation with primary antibody overnight at 4°C.

Published December 5, 2011

JEM

Cryosections were fixed with 95% ethanol and postfixed with acetone. Primary antibodies were detected with appropriate Alexa Fluor–labeled secondary antibodies (Invitrogen). All immunofluorescence images were collected and visualized with a laser-scanning confocal microscope (TCS-SP5; Leica) equipped with a 63× objective, using optical slices of 0.4–0.5 µm. Levels of images were linearly adjusted using Photoshop CS5 (Adobe).

Experimental SSSS. ETA was prepared as described previously (Hanakawa et al., 2002). Abdominal hair was removed using a depilating cream 24–48 h before the experiment. 200 µg ETA diluted in 100 µl of sterile PBS was used to challenge via i.p. injection. Abdominal skin, divided into three parts, was gently rubbed once with the right index finger 3 h after ETA challenge to observe epidermal detachment (Nikolsky's sign). The skin erosion area was quantified as several pixels, using ImagePro version 6.3 (Media Cybernetics), and this number was divided by the total pixel number of the entire abdominal area.

In vitro Dsg1 cleavage assay. A Melon Gel IgG Purification System (Thermo Fisher Scientific) was used to obtain purified IgG from sera of mice that were patch immunized with ETA or PBS. The entire extracellular domain of hrDsg1 with an E tag on the carboxyl terminus was produced as a secreted protein, using the baculovirus system as described previously (Amagai et al., 2000; Ishii et al., 1997). 20 µl of recombinant ET (4 µg/ml) was preincubated with 20 µl of purified IgG for 1 h at 37°C and then with 1 µg hrDsg1 in 10 µl PBS containing 1 mM $CaCl_2$ for 1 h. The digested samples were subjected to SDS-PAGE and transferred to polyvinylidene fluoride membranes (Bio-Rad Laboratories). Bands were detected using anti–E tag antibody and visualized with a chemiluminescent substrate (ECL Plus; GE Healthcare), followed by exposure to Kodak BioMax film (VWR international).

Statistical analysis. Statistical analysis was performed with the Student's *t* test using Prism version 5 (GraphPad Software), and p-values ≤0.05 were regarded as significant.

Online supplemental material. Fig. S1 shows the generation of mice that lack langerin$^+$ dDCs. Fig. S2 shows that the humoral response induced by LCs subsequent to ACT is restricted to IgG_1. Online supplemental material is available at http://www.jem.org/cgi/content/full/jem.20111718/DC1.

We thank Showbu Sato, Hiromi Ito, and Kayoko Eguchi for invaluable technical assistance.

This work was supported by Grants-in-Aid for Scientific Research from the Ministry of Education, Culture, Sports, Science and Technology of Japan, Research on Measures against Intractable Diseases, the Ministry of Health, Labour and Welfare of Japan, and Keio Gijuku Academic Development Funds. B.E. Clausen is a fellow of The Netherlands Organization for Scientific Research.

S. Koyasu is a consultant for Medical and Biological Laboratories Co., Ltd. The authors otherwise have no financial conflicts of interest.

Author contributions: T. Ouchi performed the majority of the experiments with assistance from A. Kubo, M. Yokouchi, T. Adachi, T. Kobayashi, D.Y. Kitashima, and H. Fujii, overseen by M. Amagai and K. Nagao. B.E. Clausen provided Langerin-DTR mice. K. Nagao conceived the experiments, and H. Fujii and S. Koyasu assisted with the BM transfer experiments. T. Ouchi and K. Nagao wrote the manuscript.

Submitted: 15 August 2011
Accepted: 2 November 2011

REFERENCES

Allan, R.S., C.M. Smith, G.T. Belz, A.L. van Lint, L.M. Wakim, W.R. Heath, and F.R. Carbone. 2003. Epidermal viral immunity induced by CD8alpha+ dendritic cells but not by Langerhans cells. *Science.* 301:1925–1928. http://dx.doi.org/10.1126/science.1087576

Amagai, M., N. Matsuyoshi, Z.H. Wang, C. Andl, and J.R. Stanley. 2000. Toxin in bullous impetigo and staphylococcal scalded-skin syndrome targets desmoglein 1. *Nat. Med.* 6:1275–1277. http://dx.doi.org/10.1038/81385

Bennett, C.L., E. van Rijn, S. Jung, K. Inaba, R.M. Steinman, M.L. Kapsenberg, and B.E. Clausen. 2005. Inducible ablation of mouse Langerhans cells diminishes but fails to abrogate contact hypersensitivity. *J. Cell Biol.* 169:569–576. http://dx.doi.org/10.1083/jcb.200501071

Bennett, C.L., M. Noordegraaf, C.A. Martina, and B.E. Clausen. 2007. Langerhans cells are required for efficient presentation of topically applied hapten to T cells. *J. Immunol.* 179:6830–6835.

Bursch, L.S., L. Wang, B. Igyarto, A. Kissenpfennig, B. Malissen, D.H. Kaplan, and K.A. Hogquist. 2007. Identification of a novel population of Langerin$^+$ dendritic cells. *J. Exp. Med.* 204:3147–3156. http://dx.doi.org/10.1084/jem.20071966

Ginhoux, F., M.P. Collin, M. Bogunovic, M. Abel, M. Leboeuf, J. Helft, J. Ochando, A. Kissenpfennig, B. Malissen, M. Grisotto, et al. 2007. Blood-derived dermal langerin$^+$ dendritic cells survey the skin in the steady state. *J. Exp. Med.* 204:3133–3146. http://dx.doi.org/10.1084/jem.20071733

Hanakawa, Y., N.M. Schechter, C. Lin, L. Garza, H. Li, T. Yamaguchi, Y. Fudaba, K. Nishifuji, M. Sugai, M. Amagai, and J.R. Stanley. 2002. Molecular mechanisms of blister formation in bullous impetigo and staphylococcal scalded skin syndrome. *J. Clin. Invest.* 110:53–60.

Ishii, K., M. Amagai, R.P. Hall, T. Hashimoto, A. Takayanagi, S. Gamou, N. Shimizu, and T. Nishikawa. 1997. Characterization of autoantibodies in pemphigus using antigen-specific enzyme-linked immunosorbent assays with baculovirus-expressed recombinant desmogleins. *J. Immunol.* 159:2010–2017.

Ishii, K., C. Lin, D.L. Siegel, and J.R. Stanley. 2008. Isolation of pathogenic monoclonal anti-desmoglein 1 human antibodies by phage display of pemphigus foliaceus autoantibodies. *J. Invest. Dermatol.* 128:939–948. http://dx.doi.org/10.1038/sj.jid.5701132

Itoh, M., S. Yonemura, A. Nagafuchi, S. Tsukita, and S. Tsukita. 1991. A 220-kD undercoat-constitutive protein: its specific localization at cadherin-based cell-cell adhesion sites. *J. Cell Biol.* 115:1449–1462. http://dx.doi.org/10.1083/jcb.115.5.1449

Kaplan, D.H., M.C. Jenison, S. Saeland, W.D. Shlomchik, and M.J. Shlomchik. 2005. Epidermal langerhans cell-deficient mice develop enhanced contact hypersensitivity. *Immunity.* 23:611–620. http://dx.doi.org/10.1016/j.immuni.2005.10.008

Kautz-Neu, K., M. Noordegraaf, S. Dinges, C.L. Bennett, D. John, B.E. Clausen, and E. von Stebut. 2011. Langerhans cells are negative regulators of the anti-*Leishmania* response. *J. Exp. Med.* 208:885–891. http://dx.doi.org/10.1084/jem.20102318

Kissenpfennig, A., S. Henri, B. Dubois, C. Laplace-Builhé, P. Perrin, N. Romani, C.H. Tripp, P. Douillard, L. Leserman, D. Kaiserlian, et al. 2005. Dynamics and function of Langerhans cells in vivo: dermal dendritic cells colonize lymph node areas distinct from slower migrating Langerhans cells. *Immunity.* 22:643–654. http://dx.doi.org/10.1016/j.immuni.2005.04.004

Kubo, A., K. Nagao, M. Yokouchi, H. Sasaki, and M. Amagai. 2009. External antigen uptake by Langerhans cells with reorganization of epidermal tight junction barriers. *J. Exp. Med.* 206:2937–2946. http://dx.doi.org/10.1084/jem.20091527

Ladhani, S., C.L. Joannou, D.P. Lochrie, R.W. Evans, and S.M. Poston. 1999. Clinical, microbial, and biochemical aspects of the exfoliative toxins causing staphylococcal scalded-skin syndrome. *Clin. Microbiol. Rev.* 12:224–242.

Merad, M., M.G. Manz, H. Karsunky, A. Wagers, W. Peters, I. Charo, I.L. Weissman, J.G. Cyster, and E.G. Engleman. 2002. Langerhans cells renew in the skin throughout life under steady-state conditions. *Nat. Immunol.* 3:1135–1141. http://dx.doi.org/10.1038/ni852

Nagao, K., F. Ginhoux, W.W. Leitner, S. Motegi, C.L. Bennett, B.E. Clausen, M. Merad, and M.C. Udey. 2009. Murine epidermal Langerhans cells and langerin-expressing dermal dendritic cells are unrelated and exhibit distinct functions. *Proc. Natl. Acad. Sci. USA.* 106:3312–3317. http://dx.doi.org/10.1073/pnas.0807126106

Nishioka, K., T. Nakano, N. Hirao, and Y. Asada. 1977a. Staphylococcal scalded skin syndrome I. Purification of exfoliatin and maternal transmission of neutralizing ability against exfoliatin. *J. Dermatol.* 4:13–18.

Published December 5, 2011

Nishioka, K., T. Nakano, N. Hirao, H. Teranishi, and Y. Asada. 1977b. Staphylococcal scalded skin syndrome. II. Serum level of anti exfoliatin and anti alpha-toxin in patients with staphylococcal scalded skin syndrome or bullous impetigo. *J. Dermatol.* 4:65–68.

Noordegraaf, M., V. Flacher, P. Stoitzner, and B.E. Clausen. 2010. Functional redundancy of Langerhans cells and Langerin+ dermal dendritic cells in contact hypersensitivity. *J. Invest. Dermatol.* 130:2752–2759. http://dx.doi.org/10.1038/jid.2010.223

Poulin, L.F., S. Henri, B. de Bovis, E. Devilard, A. Kissenpfennig, and B. Malissen. 2007. The dermis contains langerin$^+$ dendritic cells that develop and function independently of epidermal Langerhans cells. *J. Exp. Med.* 204:3119–3131. http://dx.doi.org/10.1084/jem.20071724

Prausnitz, M.R., J.A. Mikszta, M. Cormier, and A.K. Andrianov. 2009. Microneedle-based vaccines. *Curr. Top. Microbiol. Immunol.* 333:369–393. http://dx.doi.org/10.1007/978-3-540-92165-3_18

Schuler, G., and R.M. Steinman. 1985. Murine epidermal Langerhans cells mature into potent immunostimulatory dendritic cells in vitro. *J. Exp. Med.* 161:526–546. http://dx.doi.org/10.1084/jem.161.3.526

Stanley, J.R., and M. Amagai. 2006. Pemphigus, bullous impetigo, and the staphylococcal scalded-skin syndrome. *N. Engl. J. Med.* 355:1800–1810. http://dx.doi.org/10.1056/NEJMra061111

Vermeer, P.D., L.A. Einwalter, T.O. Moninger, T. Rokhlina, J.A. Kern, J. Zabner, and M.J. Welsh. 2003. Segregation of receptor and ligand regulates activation of epithelial growth factor receptor. *Nature.* 422:322–326. http://dx.doi.org/10.1038/nature01440

Wilson, N.S., and J.A. Villadangos. 2004. Lymphoid organ dendritic cells: beyond the Langerhans cells paradigm. *Immunol. Cell Biol.* 82:91–98. http://dx.doi.org/10.1111/j.1440-1711.2004.01216.x

Yager, E.J., H.J. Dean, and D.H. Fuller. 2009. Prospects for developing an effective particle-mediated DNA vaccine against influenza. *Expert Rev. Vaccines.* 8:1205–1220. http://dx.doi.org/10.1586/erv.09.82

Yamasaki, O., T. Yamaguchi, M. Sugai, C. Chapuis-Cellier, F. Arnaud, F. Vandenesch, J. Etienne, and G. Lina. 2005. Clinical manifestations of staphylococcal scalded-skin syndrome depend on serotypes of exfoliative toxins. *J. Clin. Microbiol.* 43:1890–1893. http://dx.doi.org/10.1128/JCM.43.4.1890-1893.2005

Epidermal barrier dysfunction and cutaneous sensitization in atopic diseases

Akiharu Kubo,[1,2] Keisuke Nagao,[1] and Masayuki Amagai[1]

[1]Department of Dermatology and [2]Center for Integrated Medical Research, Keio University School of Medicine, Tokyo, Japan.

Classic atopic dermatitis is complicated by asthma, allergic rhinitis, and food allergies, cumulatively referred to as atopic diseases. Recent discoveries of mutations in the filaggrin gene as predisposing factors for atopic diseases have refocused investigators' attention on epidermal barrier dysfunction as a causative mechanism. The skin's barrier function has three elements: the stratum corneum (air-liquid barrier), tight junctions (liquid-liquid barrier), and the Langerhans cell network (immunological barrier). Clarification of the molecular events underpinning epidermal barrier function and dysfunction should lead to a better understanding of the pathophysiological mechanisms of atopic diseases.

Introduction

Atopic dermatitis (AD) is a chronic relapsing eczematous skin disorder that is frequently associated with elevated serum IgE levels and a family history of AD, allergic rhinitis, and/or asthma. Clinical manifestations of classic AD are dry skin and relapsing eczema, which usually start during early infancy or childhood and become complicated by food allergies, asthma, and/or allergic rhinitis during the first several years of life, in a process called "atopic march" (1). AD is highly prevalent in industrialized countries, where it affects approximately 15%–30% of children and 2%–10% of adults (2). The various observations of the disease indicate that AD has a complex etiology with genetic, immunological, and environmental aspects.

Living organisms rely critically on surface barriers to isolate themselves from the external environment and to maintain homeostasis. While unicellular organisms are enclosed by cell membranes and cell walls, epithelial barrier structures, in several forms, cover the surfaces of multicellular organisms (3). In mammals, the airway and gastrointestinal tract are lined by simple epithelia covered with mucus. In contrast, the outer surface of the body is covered by a stratified epithelial cellular sheet called the epidermis, the outermost layer of which is cornified. Recent findings have shown that disruption of epithelial barrier systems are involved in the pathogenesis of immune disorders such as inflammatory bowel disease, asthma, and AD (4–12). In this review, we describe the barrier system of the epidermis, which is far more sophisticated than previously thought (13, 14), and attempt to discuss its function with special focus on antigen penetration through these barriers and antigen capture by dendritic cells in the context of AD.

The three musketeers of the epidermal barrier

Tight junctions as a liquid-liquid interface barrier. For cellular sheets to function as proper barriers, paracellular diffusion of fluid must be prevented. In simple, single-layer cellular sheets in vertebrates, tight junctions (TJs) are responsible for intercellular sealing and the compartmentalization of extracellular environments (ref. 3 and Figure 1A). TJs are not just physical barriers; they exhibit ion and size selectivity and their barrier function varies significantly in tightness, depending on cell type and physiological requirements, enabling dynamic regulation of substances that traffic between compartments. As a result, two adjacent compartments divided by TJ barriers can maintain different ionic strengths and solute concentrations (15–17).

Within the body of vertebrates, the TJ barrier acts as a liquid-liquid interface barrier to demarcate different fluid compartments. Examples of the compartmentalized fluids separated by TJ barriers are bile (in the lumen of bile ducts), urine (in the renal tubules), and cerebrospinal fluid (within the blood-brain barrier). TJs exist also in the body surface, both in the simple epithelia of body cavities such as intestine and trachea and in the stratified epithelia of skin. In the non-keratinized epidermis of fish and amphibian tadpoles, TJs separate the body from the external aquatic environment (18, 19). In terrestrial vertebrates, in which stratum corneum (SC) evolved presumably as an air-liquid interface barrier to avoid desiccation as animals adapted to living in contact with air, TJ barriers exist covertly under the SC barriers (18, 20–24). They compartmentalize the epidermal extracellular fluid environment into two parts in mammals (described below) and possibly also in reptiles and birds (Figure 1B).

Mammalian epidermis consists of a single layer of proliferating cells, the stratum basale, and several superficial layers of stratum spinosum and stratum granulosum (SG), which ultimately form the SC. As thin as it is, mouse ear epidermis has the minimal components of epidermal differentiation, with pre-SC cell flattening always occurring in three layers in the SG (25–27). The three SG layers are designated SG1, SG2, and SG3, counting from the surface inward. Our imaging studies of whole-mounted epidermal sheets have demonstrated that the intercellular spaces between SG2 cells are sealed by TJs (ref. 13 and Supplemental Video 1; supplemental material available online with this article; doi:10.1172/JCI57416DS1), as previously proposed based on careful observations via immunofluorescence and electron microscopy (22). Thus, SG1 cells that are about to cornify exist within a distinct fluid compartment outside of the TJ barrier, and cells below the SG2 layer are inside the barrier (Figure 1B).

The SC as an air-liquid interface barrier. As spinous layer cells differentiate into SG cells, they become flattened, with diameters up to 30 micrometers (27), and start to form lamellar and keratohyalin granules (Figure 1C). When SG3 cells differentiate into SG2 cells, they form TJs and acquire an apical-basal polarization of

Conflict of interest: The authors have declared that no conflict of interest exists.

Citation for this article: *J Clin Invest.* 2012;122(2):440–447. doi:10.1172/JCI57416.